Digital Comprehensive Summaries of Uppsala Dissertations
from the Faculty of Science and Technology 2615

Modelling and Performance of Cellular Networks

Stochastic Geometry, Queuing, and Learning Approaches

TAISIIA MOROZOVA

ACTA UNIVERSITATIS
UPSALIENSIS
2025

ISSN 1651-6214
ISBN 978-91-513-2675-7
urn:nbn:se:uu:diva-571533

UPPSALA
UNIVERSITET

Dissertation presented at Uppsala University to be publicly examined in Polhemsalen, Ångströmlaboratoriet, Lägerhyddsvägen 1, Uppsala, Wednesday, 14 January 2026 at 17:29 for the degree of Doctor of Philosophy. The examination will be conducted in English. Faculty examiner: Professor Sabine Wittevrongel (Department of Telecommunications and Information Processing, Ghent University).

Abstract
Morozova, T. 2025. Modelling and Performance of Cellular Networks. Stochastic Geometry, Queuing, and Learning Approaches. *Digital Comprehensive Summaries of Uppsala Dissertations from the Faculty of Science and Technology* 2615. 64 pp. Uppsala: Acta Universitatis Upsaliensis. ISBN 978-91-513-2675-7.

This thesis is based on seven papers concerning mathematical models for wireless cellular networks with retransmissions, buffering, and interference. The analysis combines stochastic geometry with queuing theory to capture complex stochastic aspects of the physical model. Paper I introduces a downlink model with transmitter buffers, providing performance measures such as coverage probability, delay, and loss probability. Paper II extends the modeling approach to quantify Shannon capacity under finite and infinite buffer regimes. Paper III studies multi-tier networks, extending the previous approach. The paper introduces biased load balancing and discusses the increase in capacity compared with single-tier systems. Pa-per IV derives a stability condition for buffered uplink traffic, for a special case of no noise and unbounded attenuation. The paper further refines the analytical stability bound through simulations. Paper V considers the network with heterogeneous users with different arrival rates and powers, and establishes user-specific stability bounds. Paper VI uses the well-known Foster criteria for two-dimensional Markov chains and extends them to derive both stability and transience criteria for Markov chains in higher dimensions with monotone drifts. Finally, Paper VII studies a model of a buffered cellular network in terms of reinforcement learning (RL) methodology. It introduces a decentralized mean-field RL method, where base stations act as agents who aim to maximize their channel capacity via dynamically adjusting the transmission intensity.

Keywords: Cellular networks, performance evaluation, stochastic geometry, stochastic modelling, Shannon capacity, coverage probability, Markov chains, reinforcement learning.

Taisiia Morozova, Department of Mathematics, Probability Theory and Combinatorics, Box 480, Uppsala University, SE-751 06 Uppsala, Sweden.

ISSN 1651-6214
ISBN 978-91-513-2675-7
URN urn:nbn:se:uu:diva-571533 (http://urn.kb.se/resolve?urn=urn:nbn:se:uu:diva-571533)

List of papers

This thesis is based on the following papers, which are referred to in the text by their Roman numerals.

I Ingemar Kaj and Taisiia Morozova: Retransmission performance in a stochastic geometric cellular network model. Performance Evaluation, 2024, 165, 102428, doi.org/10.1016/j.peva.2024.102428

II Ingemar Kaj and Taisiia Morozova: Channel capacity and performance analysis of a buffered cellular network. TechRxiv. September 06, 2024 (*submitted*). DOI:10.36227/techrxiv.172565778.87538590/v1

III Taisiia Morozova and Ingemar Kaj: Performance analysis and load balancing in a multi-tier buffered cellular network. in Proc. EPEW 2025, Springer Nature Computer Science (*accepted*).

IV Taisiia Morozova and Ingemar Kaj: Analysis of a typical cell in the uplink cellular network model using stochastic simulation (2022). 10.1109/CITDS54976.2022.9914210.

V Taisiia Morozova: Stability Analysis and Simulation of a Cellular Network with Retransmissions Policy (2023). Lecture Notes in Computer Science, vol 14231. Springer, Cham. https://doi.org/10.1007/978-3-031-43185-2_25

VI Illés Horváth, András Mészáros, Taisiia Morozova, Miklós Telek: Stability of multi-dimensional Markov chains with monotone drifts. 2025 (*submitted*).

VII Taisiia Morozova and Konstantin Avrachenkov: Mean-Field Multi-Agent Reinforcement Learning For Buffered Network Optimization (2025). *Manuscript*.

Reprints were made with permission from the publishers.

Contents

1 Introduction 7

2 Modeling the Spatial Structure of Cellular Networks 9
- 2.1 Rayleigh fading model 9
- 2.2 A bridge between stochastic geometry and cellular networks 10
- 2.3 Extensions to Non-Poisson models 12

3 General performance of a cellular network 14
- 3.1 Interference between the transmitters 14
- 3.2 Coverage and SINR 17
- 3.3 Shannon capacity 17

4 Delay sensitive networks 19
- 4.1 Queuing theory 19
- 4.2 Buffer process and activity of cells 20
- 4.3 Pure-loss, no-loss, and limited loss 22
- 4.4 Non-homogeneous Markov chains 25
- 4.5 Ergodicity 26

5 Multi-tier networks 27
- 5.1 System model 27
- 5.2 Path-loss laws in multi-tier framework 30
- 5.3 Interference and coverage 30

6 Networks with non-homogeneous users 32
- 6.1 System model 33
- 6.2 Ergodicity of a buffer process 34

7 Multi-dimensional Markov chains 36
- 7.1 Theoretical Tools 37
- 7.2 Buffered network with heterogeneous users as an N-dimensional MC 39
- 7.3 Assumption of monotone drifts 41

8 Dynamic optimization and reinforcement learning 43
- 8.1 Buffered Cellular Network in terms of MARL 44
- 8.2 Convergence 46

9 Summary of papers 47
- 9.1 Paper I 47

9.2 Paper II 48
9.3 Paper III 49
9.4 Paper IV 50
9.5 Paper V 51
9.6 Paper VI 53
9.7 Paper VII 54

10 Sammanfattning på svenska 55

11 Acknowledgments 56

References 58

1. Introduction

Wireless communications is a broad and emerging field that contains various technologies and applications, such as mobile networks, satellite communications, Internet of Things (IoT), and signal processing. For many years, researchers have been developing various mathematical models grounded in stochastic geometry to extensively analyze and evaluate the quality of service provided by cellular networks. These models have proven extremely important in understanding the complex interactions and behaviors within these networks, allowing for more accurate predictions and optimizations of network performance.

The studies of general cellular networks from a mathematical perspective go back to the early nineties. The most notable work was done by A. Wyner who proposed a probabilistic approach (also called a Wyner model) to describe a simple model of a cellular multiple-access system [110]. The main principle of this work is defining the channel achievable rate in terms of the Shannon formula in a network with deterministic hexagonal cells of the same size. Although the work describes an overly simplified mean-value approximation of a real-life network and allows for rather crude assumptions, it has been adopted and used as a base in capacity-focused research for many years. It has been shown in [111] that the Wyner model is indeed accurate for some special network types, namely CDMA (code-division multiple access) multi-cell networks. For this reason, the Wyner model has found applications in a lot of CDMA-related works, for example, [49, 107, 98]). The first shifts from the deterministic grid to a network with random locations were made in [91] and later developed in [14, 13, 42], where the authors propose the use of spatial stochastic processes (namely, Poisson point processes) to model the location of the nodes. In [42] the authors also suggest using the Voronoi diagram to define the edges of the cells, hence employing the shortest distance association policy. The combination of the Voronoi setting and the Poisson placement of the points results in a so-called Poisson-Voronoi framework, which allows for a tractable geometric analysis. It is shown that this approach captures the real-life placement of the base stations with a high degree of accuracy and is more efficient compared to the deterministic network structure. In the follow-up research, the approach has been extended from a two-dimensional plane to networks of higher dimensions. One of the earliest studies to investigate this extension is presented in [53], where the 3D network is studied in terms of its capacity. Some later research that continues analyzing the 3D networks includes [72, 83]. More precisely, in [83], the author focuses on stochastic

geometry techniques to capture the multi-dimensional deployment of the network. The existing research, however, lacks contributions studying networks of dimensions higher than three, for purely engineering reasoning. From an engineering standpoint, higher-dimensional networks are deemed infeasible for implementation in real-world communication systems. Nonetheless, current studies successfully characterize the topology and global dynamics of cellular networks using mathematical modeling techniques, with stochastic geometry playing a central role.

As network technologies emerged rapidly, a more sophisticated approach and modeling techniques were required to properly address the related issues such as collisions, interference, and information loss. In particular, network reliability has become a dramatic issue with the rapid growth of network density and increased traffic demand. Reliability has become the main principle of networks utilizing TCP protocols with retransmission mechanisms, where the antennas are equipped with a buffer to store the damaged information. The tools for describing the buffer dynamics in terms of a mathematical model were initially discussed in [3] and [109]. Namely, in [3], the author proposes a GI/G/1 queue model to describe a buffer process in terms of a customer's waiting time and proves its convergence. In [109], the author introduces another queueing theory approach to conduct a steady-state analysis of complex high-speed networks and to develop the concept of effective bandwidth. This approach was further developed in [24], where the author examines a similar network while also addressing the issue of effective buffer management under delay constraints.

More recent research has built on these fundamental techniques, keeping up with fast-growing model complexity and pushing the analysis further. The most relevant contributions include [4, 115, 35, 12, 92], where a comprehensive analysis of coverage probability and channel capacity is provided together with a strong physical motivation and engineering background. Some studies, including [52, 116] concentrate mostly on interference analysis and its impact on the network performance. Namely, the authors in [52] explore interference alignments, whereas [116] examines the performance of a stochastic network utilizing a successive interference cancellation (SIC) policy. Buffered systems have been analyzed in [47, 30, 78, 44], focusing on performance evaluation in TCP systems of varying complexity and proposing different delay definitions.

2. Modeling the Spatial Structure of Cellular Networks

2.1 Rayleigh fading model

A key characteristic of the physical model of a wireless network is the law governing signal attenuation as it propagates from the transmitter to the receiver. Different models have been proposed to describe the physical process of signal fading, with the Rician and Rayleigh models usually representing large-scale and small-scale fading, respectively. The Rayleigh fading model, in particular, has gained attention due to its ability to accurately characterize environments with no dominant line-of-sight (LoS) path between the transmitter and receiver, such as urban or indoor localities. The Rayleigh model was initially proposed for application to communication systems in [99, 100] where the authors used it to represent the statistical distribution of an oscillating signal amplitude. Specifically, the Rayleigh probability density function (PDF) for the amplitude of the received signal is given by

$$f(x) = \frac{x}{\sigma^2} e^{-x^2/2\sigma^2}, \quad x \geq 0, \tag{2.1}$$

where σ^2 is the variance of the underlying Gaussian random variables describing the in-phase and quadrature components of the signal. This model assumes that the transmitted signal undergoes multiple reflections and scattering, leading to a received signal that can be represented as the sum of a large number of independent, identically distributed random variables. By the central limit theorem, the received signal can be modeled as Gaussian random variables, resulting in a Rayleigh distribution. In modern research, the Rayleigh fading model is widely used to characterize signal fading in networks with a non-line-of-sight (NLoS) propagation model. Physically, an NLoS model represents a scenario where the oscillating signal is not obstructed by physical objects, such as forests or tall buildings. As a result, the signal propagation can be described by a rather simple exponential law, which allows for a tractable analysis of the model from a mathematical perspective. The Rayleigh model has been extensively validated and applied in practical systems to model different NLoS scenarios, as discussed in [4, 35]. In contrast, LoS models representing more complicated fading laws were considered in [6, 102], where the focus was on evaluating various network performance metrics, including a line-of-sight probability. Comparative studies have further highlighted the distinctions between LoS and NLoS scenarios, modeled by Rician and Rayleigh fading, respectively, as seen in [36, 15, 112]. As emphasized by the authors, the main

distinction between the two models lies in their suitability for different environmental conditions rather than any superiority or inferiority concerning network performance. These works also confirm that the Rayleigh model provides a tractable framework for analyzing and simulating fading law in wireless communication systems under realistic conditions.

2.2 A bridge between stochastic geometry and cellular networks

Various research in the field of stochastic geometry has evolved since the early nineties, providing strong methodology and tools for mathematical stochastic models, the most notable works include [101, 58]. On the engineering side, the models of cellular networks have evolved in complexity to adapt to the increased traffic demands. The two fields evolved in parallel, and at the time, there was no proper mathematical approach to capturing the complex dynamics and source allocation issues in cellular networks using stochastic geometry tools. This changed in 2011 with the release of [4], where the authors propose a tractable analytical method to describe the dynamics of a wireless cellular network. The main idea was to use the Voronoi diagram to capture the geometry of cells (see Fig. 2.1) and connect the cell association with the Shannon capacity using the results from [11]. The authors later developed their approach and adapted it to various models, including the uplink traffic model [85] and heterogeneous networks with multiple classes of BSs [62, 33]. This method has become fundamental in the field of telecommunications, and the results obtained in [4] were picked up and used in many works. The primary advantage of this approach lies in the ability to combine the properties Poisson-Voronoi framework with the Shannon formula.

To describe the key features of this framework, let us define the main settings of the proposed model. Consider two independent homogeneous Poisson point processes (PPPs) Φ_{BS} and Φ_{UE} in $\mathbb{R}^d$ representing the locations of BSs and user respectively, with intensities λ_{BS} and λ_{UE}. The spatial coverage is modeled using Voronoi cells generated by Φ_{BS}. Each Voronoi cell corresponds to the set of all points in $\mathbb{R}^d$ that are closer to a particular BS than to any other BS. A user is assumed to connect to the nearest BS, associating with the Voronoi cell containing its location. The average size of a Voronoi cell is given by $1/\lambda_{BS}$, as derived from the properties of the Poisson process [27]. The expected number of users in a Voronoi cell is therefore $\lambda_{UE}/\lambda_{BS}$, which follows from independence between Φ_{BS} and Φ_{UE}. For simplicity, the focus is made on a *typical user*, which is assumed to be located at the origin, $\{x_1, x_2, \ldots, x_d\} = \{0, 0, \ldots, 0\}$ ([4]). The probability that the typical user is assigned to the Voronoi cell of a BS located at distance r is determined by the geometric and probabilistic properties of the Voronoi tessellation. Specifically, the probability that no BS is located closer than distance r to the typical

user is given by the *null probability* of a d-dimensional homogeneous Poisson process

$$\mathbb{P}(r > R) = e^{\left(-\lambda_{BS}|B(0,1)|R^d\right)}, \tag{2.2}$$

where $|B(0,1)| = \frac{\pi^{d/2}}{\Gamma\left(\frac{d}{2}+1\right)}$ is the volume of a unit ball in $\mathbb{R}^d$. For $d = 2$, this simplifies to

$$\mathbb{P}(r > R) = e^{\left(-\pi\lambda_{BS}R^2\right)}, \tag{2.3}$$

where πR^2 is the area of a circle with radius R. Note that (2.2) and (2.3) describe the tail distribution of the distance between a typical user and its target BS in d-th and 2-nd dimension, respectively. The PDF of r is computed accordingly as

$$f_r(r) = \begin{cases} d\pi\lambda_{BS}r^{(d-1)}e^{-\pi\lambda_{BS}r^d}, r \geq 0 \\ 0, \text{ otherwise.} \end{cases}$$

To extend the analysis of a typical cell to the entire network and account for all BSs locations in Φ_{BS}, consider the random sum

$$\int_{\mathscr{C}} f(x)\,\Phi_{\mathrm{UE}}(dx) = \sum_{x_i \in \Phi_{\mathrm{UE}} \cap \mathscr{C}} f(x_i)$$

over all users within the fixed cell $\mathscr{C}$. The expected value of such sums evaluates as

$$\mathbb{E}\Big[\int_{\mathscr{C}} f(x)\,\Phi_{\mathrm{UE}}(dx)|\Phi_{\mathrm{BS}}\Big] = \lambda_0 \int_{\mathbb{R}^d} f(x)\,e^{-\lambda_1|B(0,1)||x|^d}\,dx, \tag{2.4}$$

for some integrable f ([42], $d = 2$). For a radial function, $f(x) = f(|x|)$,

$$\mathbb{E}_{\mathscr{C}}[f(X)] = \lambda_1|B(0,1)|\int_0^\infty f(u)\,e^{-\lambda_1|B(0,1)|u^d}du^{d-1}\,du, \tag{2.5}$$

see [85]. To make further analysis more convenient, we rewrite (2.5) as follows. Let

$$\ell_0 = (\lambda_1|B(0,1)|)^{-1/d}$$

and associate with the Voronoi cell $\mathscr{C}$ the corresponding Euclidean ball $B(0,\ell_0)$ in $\mathbb{R}^d$ of radius ℓ_0 and preserved expected volume $|B(0,\ell_0)| = 1/\lambda_1 = \mathbb{E}[|\mathscr{C}|]$. Then for $\ell \geq 0$, $\mathbb{P}_{\mathscr{C}}(|X| \leq \ell) = 1 - e^{(\ell/\ell_0)^d}$ and

$$\mathbb{E}_{\mathscr{C}}[f(|X|)] = \int_0^\infty f(v^{1/d}\ell_0)\,e^{-v}\,dv. \tag{2.6}$$

This thesis contains seven papers that are built upon a stochastic geometric model. We extend the classical framework by incorporating a set of novel features and propose a comprehensive approach to evaluate network performance. In the following chapter, we describe the key performance metrics, review the historical context and related research, and highlight the novel aspects of our methodology.

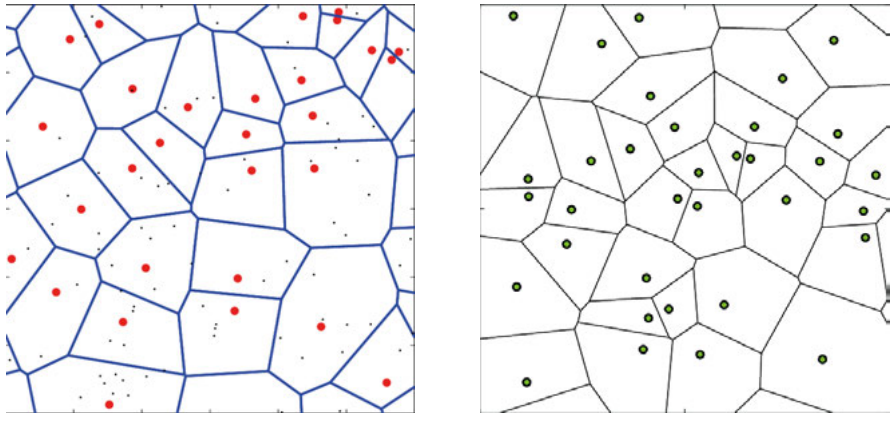

(a) *(b)*

Figure 2.1. Voronoi cells are employed to model the geometric structure of serving areas in wireless networks. The large dots represent the locations of base stations (BSs), and each cell is defined such that every point within it is closer to its associated BS than to any other BS outside the cell. Adapted from [4] and [82].

2.3 Extensions to Non-Poisson models

The Poisson process setting has become the most widely used approach in applications to spatial networks due to its simplicity and mathematical tractability. It assumes complete spatial randomness, with points located independently across space, and allows closed-form expressions for important performance metrics [55]. However, it is not the only approach to model the spatial distribution of the nodes. Empirical studies have shown that in some areas, base stations are deployed with some form of regularity, motivated by coverage optimization and interference management. To capture these features more accurately, alternative models that account for the repulsion between points have been proposed. One such model is the Ginibre point process (GPP) [32, 54]. The GPP is a determinantal point process (DPP) originally arising from random matrix theory. It is associated with the eigenvalues of complex Gaussian non-Hermitian random matrices introduced by Jean Ginibre [50]. A key property of DPPs is that their n-th order correlation functions can be expressed as determinants of a kernel function. For the Ginibre process, the joint intensity function for n points $z_1, \ldots, z_n \in \mathbb{C}$ is given by

$$\rho^{(n)}(z_1, \ldots, z_n) = \det\left[K(z_i, z_j)\right]_{1 \le i,j \le n},$$

where the kernel $K(z,w)$ is defined as

$$K(z,w) = \frac{1}{\pi} \exp\left(z\overline{w} - \frac{1}{2}(|z|^2 + |w|^2)\right).$$

This kernel creates a point process where points tend to stay apart, making it unlikely for them to be very close together. The Ginibre point process is well-suited for modeling spatial repulsion, making it more realistic than the PPP for representing base station deployments. Unlike the PPP, which allows arbitrarily close nodes, the GPP enforces spatial separation, which better fits physical constraints of the network. Studies have shown that GPP-based models yield coverage and SINR metrics more consistent with empirical data [32, 81]. The determinantal structure of the GPP allows for some analytical tractability and efficient simulation [31]. This makes it especially relevant in urban and ultra-dense networks, where infrastructure is highly concentrated, and in mmWave systems, where spatial separation is critical due to directionality and blockage.

It is worth mentioning that, despite its limitations, the PPP remains widely used in wireless network modeling. The main modeling advantage is that the PPP is mathematically simple and analytically tractable, allowing for closed-form expressions of many important performance metrics, such as coverage probability, interference distribution, and average throughput. Second, the PPP is flexible and can be easily extended to incorporate various network features, such as fading, shadowing, and user association policies. Although GPP captures spatial repulsion more realistically, it leads to more complex mathematical expressions that often require numerical methods or simulations. In scenarios where node locations are highly unpredictable or randomly deployed, such as in some ad hoc or sensor networks, the PPP is likely to provide a more appropriate and computationally efficient model.

3. General performance of a cellular network

The main goal of this thesis is to provide a performance evaluation analysis of a general class of stochastic cellular networks within the Poisson-Voronoi framework. The way such a network works is based on simultaneous transmissions of the input data between the BSs (which in practice are represented by antennas) and their associated users (mobile phones), an illustration is given in Fig. 3.1 (a). The transmission is carried out according to uplink or downlink traffic, indicating if the signal is transmitted from a BS to a user (downlink), or the opposite way (uplink), as shown in Fig. 3.1 (b). Traditionally, network systems have supported either uplink or downlink traffic at a given time. However, recent technological progress led to the development of modern full-duplex networks, which allow for simultaneous uplink and downlink traffic [70]. While these networks possess higher capabilities, the increased complexity and challenges in analytical tractability associated with full-duplex networks fall outside the scope of the current analysis. Nonetheless, certain extensions of the approach presented in this thesis could be adapted to address such systems in future studies.

The long-term dynamics of a general cellular network are characterized by a number of transmission events observed within a finite time. For analytical tractability in studying the behavior of the network, a widely adopted approach involves partitioning the total observation period into discrete time intervals of a unit length. The analysis of network performance is conducted by evaluating specific performance metrics within a time slot and examining the changes in network dynamics between the slots. The overall network performance is characterized by a collection of performance metrics and their long-term behavior. These metrics, along with their significance and implications, will be discussed in detail in the following subsections.

3.1 Interference between the transmitters

As the signal travels from a transmitter to a receiver within a cell, its quality is affected not only by the distance and physical obstacles but also by the transmissions from neighboring cells and external noise. Interference between transmitters occurs when multiple signals from different transmitters overlap, leading to signal degradation and potential information loss. The problem of interference is the main challenge in wireless networks, as it limits system capacity and affects the reliability of data transmission. In cellular networks,

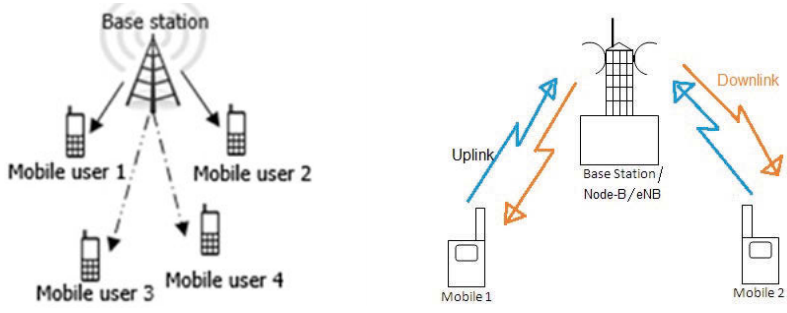

(a) *(b)*

Figure 3.1. Illustration of a cellular network with antennas (adapted from [39]) and mobile phones in the role of BSs and users, respectively. Plot (b) [88] illustrates uplink and downlink transmission in such a network.

interference can arise from co-channel transmissions, where multiple transmitters operate on the same frequency, or from adjacent-channel interference due to non-ideal frequency separation. The general interference model was initially described in [42], where the authors propose to compute the interference at the cell x as the accumulated received power from the other cells

$$I(x) = \sum_{x_k \in \Phi_x} S_k a(x_k), \tag{3.1}$$

where S is the signal power and $a(\cdot)$ is an attenuation function of a generic form

$$a(x) = \frac{1}{|x|^\beta}, x \in \mathbb{R}^d, \quad \beta > d, \tag{3.2}$$

and β is a path-loss exponent. Commonly, the signal power is represented as

$$S \sim \exp(\mu), \quad \mu \geq 0. \tag{3.3}$$

The assumption of exponentially distributed signal strength is frequently used in the analytical modeling of wireless networks, particularly when the Rayleigh fading model is employed. Providing that transmission is unaffected by shadowing and the received signal amplitude follows a Rayleigh distribution, the corresponding received power can be modeled as an exponential distribution [4]. This result comes from the mathematical properties of the Rayleigh distribution (2.1), where the square of the amplitude (representing power) inherently follows an exponential distribution.

Expression (3.2) represents the simplest attenuation law where the dependence is only on the node location and pathloss exponent. In the specific case where the transmitter is located at a unit distance from the origin ($x = 1$), the

attenuation becomes

$$a(1) = 1. \tag{3.4}$$

This choice ensures that, at a unit distance, the transmitted signal experiences no attenuation, resulting in the received power being equal to the transmitted signal power. This is a natural property of a signal, whereby it preserves its original strength while propagating over a normalized unit distance. However, a common issue and a matter of discussion related to (3.2) is its singularity in 0 as $a(0) = \infty$. Physically, this implies that if a node is positioned extremely close to the serving station (such that the distance can be considered negligible), the signal transmitted from the node would exhibit infinite strength. This results in a so-called unbounded path loss model (UBM). These models are widely used in telecommunications research and have been extensively analyzed in the literature, see, for example, [57]. Although such models provide analytical simplicity and are suitable for deriving tractable results, they fail to account for key physical and environmental constraints of real-world scenarios. In practice, signal power cannot decrease below the thermal noise floor, leading to a bounded minimum received power. UBMs do not impose such a bound, resulting in unrealistic attenuation for close distances. Additionally, communication systems often operate within finite coverage areas, beyond which the signal becomes undetectable. UBMs, by definition, neglect this limitation. As a result, while UBMs are important for theoretical analysis, their limitations motivate the use of more realistic models, such as bounded path loss models (BPM) or hybrid approaches. For this reason, different variations of the model (3.2) are employed to account for more realistic attenuation. These variations often include the addition of a unit to the denominator to eliminate the singularity at $x = 0$. Then attenuation is given by

$$a(x) = \frac{1}{1 + |x|^{\beta}}, \tag{3.5}$$

as was proposed, for example, in [74, 45]. The issue with (3.5) is that the special case of unit distance yields $a(1) = 1/2$, hence the received signal is weaker than the transmit power. This violates the assumption (3.4), resulting in an impractical attenuation rule. To combine the advantages of (3.2) and (3.5), we introduce a different attenuation law as

$$a_{\kappa,\beta}(x) = \frac{1 + \kappa}{\kappa + |x/r_0|^{\beta}}, \tag{3.6}$$

where $\kappa > 0$ is a tuning parameter and r_0 is the radius of the unit ball $B(0, r_0)$ in dimension d. The choice of this attenuation rule is motivated by the cell-based network design. Namely, attenuation (3.6) possesses the two significant properties. Specifically, $a_{\kappa,\beta}(0) = (1 + \kappa)/\kappa < \infty$ ensuring the absence of singularity at $x = 0$, and $a_{\kappa,\beta}(1) = 1$, indicating that the attenuation is appropriately adjusted to the cell size.

3.2 Coverage and SINR

As the signal is significantly affected by various effects such as fading and interference, its quality is evaluated based on the combined impact of these factors and the strength of the signal itself. The Signal-to-Interference-plus-Noise Ratio (SINR) is a critical performance metric in wireless communication systems, where it quantifies the quality and reliability of a communication link. Mathematically, the SINR of a transmitter located at x can be expressed as

$$\mathrm{SINR}(x) = \frac{Sa_{\kappa,\beta}(x)}{I(x)+\sigma^2}, \tag{3.7}$$

where S is the received power, $I(x)$ is the total interference, and σ^2 is the noise power, typically modeled as additive white Gaussian noise. The estimated value of the SINR is crucial in determining the achievable data rate and overall signal quality of a transmitter. A higher SINR generally corresponds to better service quality and hence a reliable transmission. The concept of SINR was first introduced in the early studies of wireless communications and cellular systems, with its roots starting in the late 1940s (see [97, 89]). In the context of cellular networks, SINR is particularly significant for determining the *coverage probability*, which is defined as

$$V_T(x) = \mathbb{P}(\mathrm{SINR}(x) > T). \tag{3.8}$$

To put into words, the expression (3.8) is the probability that SINR at a given receiver exceeds some predefined threshold $T > 0$ resulting in successful transmission of a given signal. The critical threshold is set according to the requirements of the communication system, such as maintaining a specific bit error rate (BER) or supporting a target data rate. A common choice of the critical threshold is $T = 1$, which indicates that a signal is successfully transmitted whenever its strength exceeds the combined strength of interference and additional noise. Studies of cellular networks typically include either numerical or analytical evaluations of the coverage probability, and based on its properties, the network performance is assessed. Paper I presents a comprehensive analysis of coverage probability under various model settings, drawing on analytical, numerical, and simulation results.

3.3 Shannon capacity

Another key performance metric is the network's channel capacity. The Shannon formula, introduced by Claude E. Shannon in his work on information theory in 1948 [97], has since then been used to describe a fundamental concept in telecommunications that quantifies the channel capacity. More precisely, this metric corresponds to the maximum achievable data transmission rate over a communication channel under given constraints, while maintaining

a low error probability. The formula for the channel capacity in terms of the Shannon formula (further addressed as Shannon capacity) of an additive white Gaussian noise channel is given by

$$C = B\log_2\left(1+\frac{P}{N_0 B}\right), \tag{3.9}$$

where C is the channel capacity in bits per second, B is the channel bandwidth in Hertz, P is the transmitted signal power, and N_0 is the noise power spectral density. The main motivation for introducing Shannon capacity from an engineering perspective was to provide a framework for understanding the trade-offs between data rate, bandwidth, and noise in communication systems. From a mathematical perspective, the concept of Shannon capacity is based on probabilistic and statistical principles. In cellular network analysis, the Shannon capacity is often expressed in terms of the SINR and is defined as

$$C = \mathbb{E}[B\log_2(1+\mathrm{SINR}(x))]. \tag{3.10}$$

The main motivation of this idea is to extend the classical concept introduced by Shannon to network environments where interference is a dominant factor affecting network performance. To further relate Shannon capacity with the corresponding coverage probability, we propose to re-write (3.10) using an integral representation of a logarithmic function as

$$\begin{aligned} C &= \mathbb{E}[w\log_2(1+\mathrm{SINR}(x))] \\ &= \frac{w}{\ln 2}\mathbb{E}\Big[\int_0^{\mathrm{SINR}(x)}\frac{1}{1+t}\,dt\Big]. \end{aligned} \tag{3.11}$$

Paper II mainly focuses on the Shannon capacity and provides analytical and numerical analysis of the capacity for different system constraints.

4. Delay sensitive networks

Building on a general model of a stochastic network, we rely heavily on the engineering perspective concerning modern wireless communications. Reliability is a critical aspect of wireless technologies, particularly in cases when data loss or corruption can significantly impact communication performance (for example, a conversation over a mobile phone). Reliability problems are normally caused by factors such as interference, fading, and congestion. One commonly employed approach to increase reliability involves the use of virtual buffers, which store incoming data packets temporarily to compensate for packet loss and interruptions in network conditions. This mechanism is employed by several communication protocols, for instance, the Transmission Control Protocol (TCP). This protocol uses retransmission buffers to ensure that lost packets are resent [61]. Similarly, the Radio Link Control (RLC) layer in Long-Term Evolution (LTE) networks utilizes buffers to manage retransmissions at the link level, preventing excessive packet loss [68]. The retransmission mechanism provides a high reliability level but naturally leads to higher latency, which is a crucial performance indicator for multiple types of delay-sensitive networks. Such networks normally demand strict latency constraints, and the extensive buffering becomes impractical. It is the case in many applications, such as real-time video streaming, VoIP, and industrial automation, where large buffering can significantly degrade performance [26]. Protocols designed for such networks, including the Quick UDP Internet Connections (QUIC) protocol and 5G Ultra-Reliable Low-Latency Communication (URLLC), prioritize low-latency transmission over loss recovery [94]. From a mathematical perspective, an accurate evaluation of such a network's performance critically depends on developing a precise mathematical model of the buffering mechanism.

4.1 Queuing theory

A set of strong mathematical tools for modeling and analyzing an accumulated stochastic process and studying its dynamics over time is provided by queuing theory. A queuing system is typically described by Kendall notation $A/S/c$, where A represents the arrival process, S denotes the service time distribution, and c is the number of servers. The simplest and most studied queuing model is the $M/M/1$ queue, which assumes a Poisson arrival process with rate λ and an exponential service time distribution with rate μ. A fundamental concept

in queuing theory is the queuing process $Q(n)$, which represents the number of packets in the system at time n. Most of the queuing theory-based approach is targeted towards analyzing the stationary distribution of $Q(n)$ and studying its behavior under various network parameters.

In practical applications, multiple queues are interconnected, forming queuing networks. These networks can be classified into open and closed systems. An open queuing network allows customers to enter and exit the system, while a closed network has a fixed number of customers circulating within it [65]. In the context of wireless communications, an open queuing model is preferred, as transmitting nodes continuously obtain and transmit newly acquired information. The network is then equipped with one or multiple buffers, which are used to store data packets awaiting transmission. The dynamics of the accumulated data packets in a single-server queue is usually described by the Lindley recursion

$$B_{n+1} = \max(0, B_n + A_n - S_n), \tag{4.1}$$

where B_n represents the size of the buffer at slot n, A_n is the inter-arrival time, and S_n is the service time. Various queuing models, such as M/M/1, M/M/c, and M/G/1, have been employed to analyze different traffic scenarios [65]. The queuing theory-based approach is usually used to evaluate performance metrics such as packet delay, loss probability, and throughput (see, for example, [9]).

4.2 Buffer process and activity of cells

The overall performance of a network is typically assessed based on the long-term efficiency of data transmissions. In physical systems, a transmission originates from a data packet of a specified length, which is generally encoded into signals. The arrival process of signals is often modeled using stochastic processes to capture the randomness in wireless environments, common models include the Poisson process [66] and Markov Chains [106]. The modeling approach depends strongly on the network structure and properties. For example, in slotted ALOHA, time is divided into discrete slots of equal length, and each station is allowed to transmit only at the beginning of a time slot. A mathematical model of such a network typically assumes that a BS transmits signals with some predefined probability, which remains the same across the time slots. It is then common to model the incoming signals via Bernoulli process as was done, for example, in [87, 90]. Another approach is to model the system under saturated assumptions, which corresponds to the case where every antenna obtains a new single at each time slot with probability 1 [4].

We use a similar approach as in [87, 90] and assume that new traffic enters the system according to a random process, where, in each discrete time slot, any given transmission link is requested to accommodate a new signal

with probability p, $0 \leq p \leq 1$. The arrivals are assumed to be independent across both time slots and transmitters. Hence, each user (UE) independently requires a link establishment with probability p, which is assumed to be sufficiently small. The BS selects a UE uniformly distributed within the cell with probability

$$\rho = \frac{p\lambda_{UE}}{\lambda_{BS}} < 1,$$

which represents the expected service load per time slot. Thus, an indicator variable $A_n \sim \text{Bin}(1,p)$ represents the occurrence of a newly generated transmission signal for a chosen BS at time slot n. To characterize the retransmission dynamics, each transmitter is associated with a buffer mechanism that stores signals corresponding to unsuccessful transmissions and schedules their retransmission at the earliest available time slot. Let B_n denote the number of buffered signals at a typical link, while B_n^k represents the buffer occupancy of an interferer located at $x_k \in \Phi_x$. The presence of the buffer significantly impacts the model's properties as it introduces the notion of nodes *activity*. To refine the model specification, we define the notation of *active* and *idle* cells. An *active* cell corresponds to a BS that has buffered or newly received signals awaiting transmission, whereas an *idle* cell represents a BS with no active jobs. Formally, the activation of the base station at x_k in slot n corresponds to the event

$$A_n^k + B_{n-1}^k \geq 1.$$

This condition holds if a new transmission is initiated (then $A_n^k = 1$) or if at least one previously unsuccessful transmission remains buffered (then $B_{n-1}^k \geq 1$). The interference at the receiver is the aggregated signal power contributed by all active emitters. Consequently, the interference expression given in (3.1) can be rewritten as

$$I_n(0,x) = \sum_{x_k \in \Phi_x} S_n^k a(x_k) \mathbf{1}_{\{\text{BS at } x_k \text{ is active}\}}, \tag{4.2}$$

where $S_n^k \sim \exp(\mu)$, according to (3.3). The key distinction between (3.1) and (4.2) is the inclusion of the indicator function, which accounts for active links and leads to the whole expression being dependent on n. To ensure the analytical tractability of the model while preserving its main characteristics, we introduce a simplified approximation that facilitates further analysis. Let us re-define the interference formula as

$$\mathscr{I}_n(x) = \sum_{x_k \in \Phi_x} Q_n^k S_n^k a(x_k), \tag{4.3}$$

where $Q_n \sim \text{Bin}(1,q_n)$ and $\{Q_n^k \sim \text{Bin}(1,q_n)\}_{x_k \in \Phi_x}$ are mutually independent Bernoulli random variables. The parameter q_n, satisfying $q_n \geq p$, serves as a mean-field approximation for the probability set

$$\{\mathbb{P}(A_n + B_{n-1} \geq 1), \mathbb{P}(A_n^k + B_{n-1}^k \geq 1), x_k \in \Phi_x\},$$

which is the steady-state probability of a busy link during slot n. Formally, q_n depends on the buffer distribution B_n and is defined as

$$q_n = 1 - (1-p)\mathsf{P}(B_n = 0).$$

Paper I provides a comprehensive analysis of the properties and asymptotic behavior of the sequence q_n. Specifically, we establish the existence of a limiting value for q_n as n grows large, given by

$$q^* = \lim_{n\to\infty} q_n. \tag{4.4}$$

Furthermore, we analyze the sequence q_n, its convergence properties, and the limiting distribution of the associated buffer size B_n. Subsequently, we derive conditions under which the sequence q_n converges and explore the implications of this convergence on the stationary distribution of B_n.

4.3 Pure-loss, no-loss, and limited loss

Depending on the buffer configurations at the BSs and mobile devices, network performance varies significantly, particularly in terms of delay, packet loss, and throughput. In this context, cellular networks can be classified into three major categories: (i) networks with finite buffers that allow both retransmissions and losses, (ii) networks with infinite buffers allowing retransmissions without losses, and (iii) networks with no buffering mechanisms (see Fig. 4.1). Each configuration influences the reliability of data transmission, and several protocols have been designed to optimize performance under different buffer configurations. Let $K \geq 0$ denote the maximum number of signals that can be concurrently stored in the buffer and let

$$Z_n = \mathbf{1}_{\{\mathrm{SINR}_n(x) > T\}}, \quad n \geq 1, \tag{4.5}$$

be the indicator of successful transmission. To accurately characterize the evolution of the buffer state at slot n, a recursion (4.1) is adopted and specifically tailored to the buffer configuration.

In practical deployments, cellular networks are often constrained by limited buffer sizes at both the BS and UE. Finite buffer sizes impact the network's ability to handle bursty traffic, leading to potential packet losses due to buffer overflows. In such systems, the problems of reliability and latency trade-off are of high importance, as discussed, for example, in [75, 2]. Some retransmission mechanisms, such as those implemented in protocols like Hybrid Automatic Repeat reQuest (HARQ) and Automatic Repeat reQuest (ARQ), can resent lost packets, hence mitigating the downside effects of finite buffers. LTE and 5G New Radio (NR) employ HARQ, which combines forward error correction with retransmission strategies [17, 60]. The effectiveness of

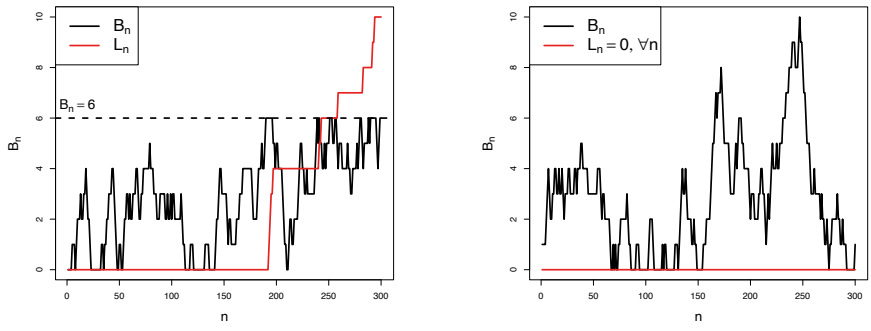

(a) *(b)*

Figure 4.1. Illustration of a buffer process and accumulated losses over $n = 300$ time slots. Plot (b) illustrates the no-loss case when $K = \infty$, where a packet loss is not possible, and plot (a) illustrates the buffer and losses for the case when $K = 6$.

HARQ depends on buffer capacity. When the buffer is full, incoming packets may be dropped, requiring higher-layer retransmissions, such as those in the Transmission Control Protocol (TCP).

Employing the finite buffer mechanism in a mathematical model typically does not allow for higher-level retransmissions, which can hinder the traceability of the analysis. It means that if a newly arrived signal meets a full buffer, the data is permanently lost. In this case, the Lindley-type recursion for the buffered signals at slot n takes the form

$$B_n = B_{n-1} + A_n \cdot (1 - \mathbf{1}_{\{B_{n-1}=K\}}) - Z_n, \quad n \geq 1, \tag{4.6}$$

where $B_n = 0$, indicating that a buffer of a typical node is always empty at the beginning of service. Similarly, the process $(L_n)_{n\geq 0}$ of accumulated lost signals is defined as

$$L_n = L_{n-1} + A_n \cdot \mathbf{1}_{\{B_{n-1}=K\}}, \quad n \geq 1, \tag{4.7}$$

with $L_0 = 0$. Consequently, the buffer level is characterized by the following dynamics. Whenever an incoming signal arrives and is not discarded, but the transmission attempt fails, the failed signal is stored in an associated buffer of the transmitting BS. Hence, the buffer size increases by one unit. In contrast, the buffer decreases by one unit if either no new signal arrives or an arriving signal is lost, provided that a previously stored signal is successfully transmitted.

Theoretical models often assume infinite buffer sizes to simplify performance analysis and provide upper bounds on network efficiency. An infinite buffer model allows all incoming packets to be stored indefinitely, eliminating packet loss due to buffer overflow but potentially introducing excessive queuing delays. Such systems are addressed as *no-loss*, and the retransmissions

operate under the assumption that all lost packets can be recovered given sufficient time. This scenario is especially relevant in idealized analytical studies of queuing systems, such as M/M/1 or M/G/1 queues with retrial capabilities [108, 7]. Although practical implementations do not feature truly infinite buffers due to physical and energy constraints, such models are interesting from an analytical perspective. The Lindley-type recursion for an infinite buffer is written as

$$B_n = B_{n-1} + A_n - Z_n, \quad n \geq 1, \quad B_0 = 0. \tag{4.8}$$

In this case, the stability of the buffer process can be analyzed using the classical *negative drift* condition ([95]), i.e.

$$\mathbb{E}A_n - \mathbb{E}Z_n = 0, \qquad p \leq V_T(q_n). \tag{4.9}$$

Within the framework of queuing theory, the negative drift implies that the arrival rate remains below the service rate. In the context of a cellular network employing the ALOHA protocol, this criterion implies that the arrival probability p does not exceed the coverage probability $V_T(q_n)$.

At the other extreme, a wide class of networks does not possess any retransmission mechanism. These systems are addressed as *pure-loss*, where the network discards incoming signals if immediate transmission is not possible. This configuration is typical in ultra-reliable low-latency communications (URLLC) scenarios, where minimal delay is a higher priority than packet delivery [18]. Without buffering, retransmission mechanisms are significantly constrained, leading to the need for alternative reliability techniques such as diversity schemes and erasure coding. Protocols such as Grant-Free Access in 5G NR enable ultra-fast transmission by avoiding conventional scheduling and queuing [69]. This approach is particularly beneficial for time-sensitive applications, such as industrial automation and vehicular networks.

In the framework of the observed model, since the system does not implement any retransmission mechanism, a BS is considered active only when a new signal is obtained. As a consequence, the probability that the link is busy is equal to the arrival probability, p, which remains constant across time slots, i.e.,

$$q_n = p, \quad \text{for all } n \geq 0.$$

The evolution of the accumulated losses $(L_n)_{n\geq 0}$ is given by the recursive relation

$$L_n = L_{n-1} + A_n - Z_n, \quad n \geq 1, \quad L_0 = 0. \tag{4.10}$$

Since the system does not allow for retransmissions, any signal that is not successfully transmitted is immediately classified as lost. Consequently, the difference $A_n - Z_n$ can only take the values 0 or 1, indicating that in any given slot either no signal is lost (when $A_n = Z_n$) or exactly one signal is lost (when $A_n = 1$ and $Z_n = 0$). This constraint comes from the assumption that at most one signal can be lost in each slot.

4.4 Non-homogeneous Markov chains

The key parameters of the observed model are the activity probability and the limiting distribution of the associated buffer size. To properly evaluate the network's performance, the analytical derivation of q_n and B_n is in order. Since both terms depend on n, the model becomes time-inhomogeneous. This complication can be handled using fundamental results from the theory of non-homogeneous Markov chains (MC). This framework allows for characterization of the long-term system's behavior by examining its transient dynamics and eventual stabilization. General Markov chains are characterized by the Markov property. Consider a discrete state space S and a sequence of random variables $\{X_n\}_{n\geq 0}$ taking values in S. The Markov property for this process can be written as

$$\mathbb{P}(X_{n+1} = j \mid X_n = i, X_{n-1} = i_{n-1}, \ldots, X_0 = i_0) = \mathbb{P}(X_{n+1} = j \mid X_n = i),$$

for all $n \geq 0$ and for all states $i, j \in S$ and any sequence $i_0, i_1, \ldots, i_{n-1} \in S$. Typically, a Markov chain is characterized by a transition matrix

$$\mathbf{M} = \{p_{ij}\} = \{\mathbb{P}(X_{n+1} = j \mid X_n = i)\},$$

which describes the transition probabilities between steps $i, j, \forall i, j \in S$ at any time step. In the non-homogeneous setting, the one-step transition probability explicitly depends on time and is defined as

$$p_{ij}(n) = \mathbb{P}(X_{n+1} = j \mid X_n = i).$$

The literature addressing the properties of non-homogeneous Markov chains is relatively limited. The most notable contributions in this area include [59] and [23], where ergodicity conditions are rigorously analyzed. A more recent contribution features the work [105], which is mainly devoted to various applications of time non-homogeneous MC. Such models are particularly useful in modeling situations where the system dynamics evolve over time. For example, in finance, market conditions change due to external economic factors, making the probabilities of moving between different market states (such as bull or bear markets) time-dependent. (see for example [86], where a regime-switching Markov chain (RSMC) is applied to model the time series of the sovereign credit rating, and the superiority of RSMC over the homogeneous MC is discussed.)

To connect the MC theory with the observed network model, we highlight key properties of the buffer process B_n. From the recursions in (4.6),(4.8), it follows that B_n depends only on B_{n-1}, making the earlier history irrelevant. The process changes by at most one unit per time slot, and thus forms a discrete-time jump process of birth-death type [96, 29]. Accordingly, $\{B_n\}_{n\geq 0}$ is a discrete-time non-homogeneous birth-death Markov chain with time-dependent transition probabilities determined by the busy link probabilities q_n. These

probabilities construct a transition matrix

$$\mathbf{M_n} = p_n(i,j),$$

which is updated in response to the current busy link probabilities q_n, which in turn are determined by the aggregate state of the system.

4.5 Ergodicity

To carefully analyze the nonlinear recursion that arises from the time dependency, a classical result from Markov chain theory [59] can be used. A non-homogeneous Markov chain with an associated sequence of transition matrices $(\boldsymbol{M}_n)$ is said to be strongly ergodic if there exists a probability distribution π such that for all $m \geq 1$,

$$\lim_{n\to\infty} \sup_{\mu} d_{TV}(\mu(\boldsymbol{M}_m \times \cdots \times \boldsymbol{M}_n), \pi) = 0, \tag{4.11}$$

where $d_{TV}(\mu,\nu)$ is total variation distance between probability distributions on $\{0,\ldots,K\}$ and the supremum is over all such distributions [23, Def. 8.2]. This result allows for verifying that the resulting time non-homogeneous buffer Markov chain is strongly ergodic. In this context, strong ergodicity implies that the distribution of the Markov chain converges to a unique invariant distribution irrespective of the initial state, and the convergence occurs at a uniform rate over all starting conditions.

Paper I analyzes the convergence of q_n and proves the existence of the stationary limit q^* for cases $K = \infty$ and $K < \infty$ for general values of σ^2 and κ. Consequently, the paper contains proof of ergodicity and the explicit form of the buffer distribution B_n. Paper IV provides the ergodicity results for the special case $K = \infty$ and $\kappa = \sigma^2 = 0$ 3.5), (3.7). In this case, the respective stability condition is obtained as an upper bound of the input traffic p using the negative drift condition (4.9).

5. Multi-tier networks

The growth of wireless data traffic, driven by an increased number of mobile devices and data-intensive applications, demands advanced network architectures. Multi-tier (heterogeneous) networks, or HetNets, address this need by integrating macro cells with low-power nodes such as micro, pico, and femtocells, [5] (see Fig. 5.1). HetNets are particularly effective in dense urban environments, forming the base of LTE-Advanced (LTE-A) and 5G deployments. Applications include high-capacity urban hotspots, where small cells offload traffic from macro cells, and smart cities, where multi-tier designs support IoT applications with reduced latency and improved reliability [46]. Modern standards such as LTE-A's enhanced Inter-Cell Interference Coordination (eICIC) and 5G's Ultra-Reliable Low-Latency Communication (URLLC) optimize resource allocation and interference management [1]. Additionally, Device-to-Device (D2D) protocols enable direct communication between nearby users, further lowering latency and easing core network load [8].

The concept of multi-tier networks is based on the principles of densification and heterogeneous deployment. The theory is based on stochastic geometry and builds a mathematical framework to analyze spatial distributions of BS and users [34]. A crucial theoretical aspect of such networks is the trade-off between network densification and interference management. As more tiers are added, the potential for co-channel interference increases, necessitating efficient interference mitigation techniques, such as interference coordination and cancellation [12].

5.1 System model

In the multi-tier setting, the foundational stochastic geometry assumptions remain consistent with those of the single-tier case. However, the multi-tier structure introduces additional complexity due to the heterogeneity in the characteristics of each tier, such as transmit power, density, and deployment strategy. Consistent with the single-tier case, we consider a heterogeneous wireless network deployed in a d-dimensional Euclidean space $\mathbb{R}^d$. The network consists of $J \geq 1$ tiers of BSs, each corresponding to different network layers (e.g., macro, micro, pico, and femtocells), and a single class of users. Data transmission is assumed to occur in the downlink direction, where BSs serve UEs located within their respective transmission cells. To mathematically characterize the spatial randomness inherent in the deployment of BSs and UEs, we

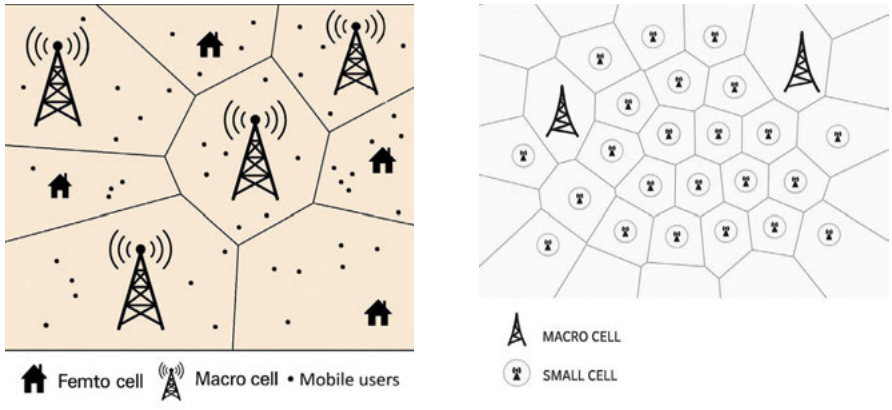

(a) *(b)*

Figure 5.1. Illustration of the multi-tier network deployment where multiple classes of BSs are present.

adopt the familiar Poisson point process framework. Formally, let

$$\Phi = \{\Phi^1, \ldots, \Phi^J\}, \quad \Phi^i \sim \text{PPP}(\lambda_i), \quad i = 1, \ldots, J,$$

denote the collection of independent homogeneous PPPs representing the spatial distribution of BSs in each of the J tiers. Here, $\lambda_i > 0$ denotes the intensity (average number of points per unit volume in $\mathbb{R}^d$) of tier-i BSs. Similarly, the spatial distribution of UEs is modeled as an independent homogeneous PPP:

$$\Phi_{\text{UE}} \sim \text{PPP}(\lambda_0),$$

where $\lambda_0 > 0$ represents the intensity of UEs in $\mathbb{R}^d$. The assumption of homogeneous PPPs for both BSs and UEs is motivated by their analytical convenience and suitability for large-scale network modeling. The processes Φ^i and Φ_{UE} are assumed to be mutually independent for all $i = 1, \ldots, J$. The total BS intensity is $\lambda = \sum_{i=1}^{J} \lambda_i$. The system bandwidth per user is defined as

$$\omega = \frac{\lambda_0}{\lambda},$$

which represents the average number of users per BS. In multi-tier wireless networks, BSs belonging to different tiers are primarily distinguished by their transmission power, coverage radius, and deployment density. Macrocells typically represent the top tier in the network hierarchy, with BSs operating at high transmission powers (20-40 W), enabling coverage over large areas with radii ranging from 1 to 20 km [38]. In contrast, small cells are represented by micro, pico, and femtocells, and are characterized by lower transmission powers and smaller coverage areas. Microcells, with power levels of a few

watts and radii of several hundred meters, are deployed in urban environments to offload macrocell traffic. Picocells, covering tens of meters, serve localized areas such as malls and offices, while femtocells operate at 100 mW and typically cover less than 10 meters, targeting residential or small-office settings [19]. These tiered deployments are strategically designed: macrocells handle wide-area coverage, while small cells reduce user-to-BS distances and improve SINR and data rates, especially in high-density regions [48].

Analogous to the single-tier network scenario, signal transmissions in the multi-tier network framework are assumed to occur in discrete time slots. In each time slot, a tier-i BS generates a new signal with probability p and transmits it with power

$$S_i \sim \text{Exp}(\mu_i), \quad 1 \leq i \leq J.$$

Regular BSs exhibit the highest signal power levels, with signal strengths decreasing progressively across subsequent tiers, that is

$$\mu_1 \leq \mu_2 \leq \cdots \leq \mu_J. \tag{5.1}$$

The ordering of tiers reflects a systematic reduction in signal power, influenced by transmission power constraints, path loss, and interference levels. This assumption aligns with practical deployments in heterogeneous wireless networks. Users are associated with the BS providing the shortest Euclidean distance, independent of transmission power. Consequently, the network partitions into Poisson-Voronoi cells of intensity λ, each having an expected volume of $1/\lambda$. The probability that a typical UE at the origin is served by a tier-i BS is given by

$$\alpha_i = \frac{\lambda_i}{\sum_{j=1}^{J} \lambda_j}. \tag{5.2}$$

Similar to the single-tier scenario, the shortest-distance association policy is adopted to establish connections between users and their serving BSs. Consequently, in a multi-tier heterogeneous network, a denser deployment of BSs in tier i significantly increases the probability that users will associate with this particular tier. However, the scope of multi-tier network analysis extends beyond the shortest-distance association assumption. An alternative and widely adopted association rule is the *strongest-received-power association policy*. Under this approach, users connects to the BS that delivers the maximum received signal power, regardless of physical distance. This policy accounts for transmit power differences across tiers, shadowing, and fading effects, which may cause users to prefer more powerful but geographically distant BSs [104]. This policy is particularly relevant in networks where small-cell deployment exceeds that of macro cells. Hybrid association policies that combine distance-based and power-based criteria have also been explored in the literature. For instance, biasing techniques, where additional bias factors are applied to received power levels from small cells, have been proposed to encourage offloading from macrocells [62, 73].

5.2 Path-loss laws in multi-tier framework

In both single-tier and multi-tier scenarios, the primary fading mechanism affecting signal propagation is often modeled using Rayleigh fading (2.1). The corresponding signal attenuation is modeled according to the bounded path-loss function defined in (3.6).

In theoretical studies of multi-tier cellular networks, a common simplifying assumption is the use of the same path-loss exponent β across all tiers [33]. Under this assumption, the attenuation of a typical signal is considered identical regardless of the tier of the serving BS. This approach, however, does not properly reflect the heterogeneous nature of the network. In particular, as discussed in [62], applying the same path-loss exponent to all tiers does not significantly affect network performance, especially in dense deployments involving femtocells and microcells. The reason lies in the increased overall interference resulting from the proximity of low-power BSs, which cancels the expected benefits of network densification. To address this limitation, it has been proposed that tier-specific path-loss exponents be adopted [76, 20]. Specifically, BSs of more powerful tiers are modeled with smaller path-loss exponents. This choice is consistent with propagation conditions where signals experience lower attenuation over longer distances. Similarly, femtocells and microcells are assigned higher path-loss exponents to capture rapid signal attenuation observed in low-scale locations [48].

5.3 Interference and coverage

Similarly to the single-tier case, a typical UE is assumed to be located at the origin. In a multi-tier heterogeneous network scenario, the SINR expression must be adapted to account for the presence of multiple tiers. The heterogeneity introduces additional complexity in the interference characterization, as interference now originates from BSs across all tiers. Hence, the interference expression (3.1) defined for the single-tier case is modified accordingly and becomes

$$\mathscr{I}(x) = \sum_{j=1}^{J} \sum_{y \in \Phi^j \setminus x} a(y) S_y^{(j)} Q_y^{(j)}, \tag{5.3}$$

where $a(\cdot)$ is defined as in (3.6). In other words, the total interference consists of active transmitters of each tier. Here, $\{Q_y^{(j)}\}$ is a family of independent random variables, such that $Q_y^{(j)} \sim \mathrm{Bin}(1, q_j)$ and q_j is the probability that a link in tier j is active, for each $y \in \Phi^j$ and $1 \le j \le J$. Consequently, the SINR and the respective coverage probability for the tier i is

$$\mathrm{SINR}^{(i)}(x) = \frac{a(x) S^{(i)}}{\mathscr{I}(x) + \sigma^2}, \qquad V_{T_i}^{(i)}(q) = \mathbb{E}[\mathbb{P}(\mathrm{SINR}^{(i)}(x) > T_i)].$$

where x is the cell location of the BS, σ^2 is a constant noise contribution and T_i is the tier-specific critical threshold. In the analysis of multi-tier wireless networks, it is often assumed that the SINR threshold T remains identical across all transmitters, regardless of the tier to which they belong [34]. However, this assumption may not accurately capture practical deployment scenarios. Moreover, under this assumption, the additional deployment of lower-tier BSs, such as microcells and femtocells, does not significantly affect the network performance in terms of coverage probability [34]. In real-world heterogeneous networks, macrocell BSs typically provide significantly larger coverage areas and higher transmission powers compared to smaller cells [76]. Consequently, it is more realistic to assign higher SINR threshold values to macrocells due to their ability to provide reliable communication over long distances. On the other hand, smaller cells possess weaker signal strengths due to lower transmission powers and limited coverage areas. Allowing high SINR thresholds on such cells may lead to increased transmission failures, as the received signal power may not suffice to meet the SINR requirements [20, 62]. Therefore, it is beneficial to adopt a threshold design such that T_i decreases with the tier i level. This tier-dependent SINR threshold strategy also aligns with resource management techniques and interference mitigation strategies typically employed in modern wireless networks [28, Chapter 8.7].

Paper III provides an analysis of a multi-tier network with a focus on coverage probability, Shannon capacity, and the characterization of tier-specific busy probabilities $q_n^{(i)}, 0 < j \leq J$. The main idea of the approach is the assumption of *biased load balancing*, where the signal power and the critical threshold are balanced across tiers. This leads to the activity probability q_i being identical for every tier.

6. Networks with non-homogeneous users

The analyses in Chapters 2-4 are based on the simplifying assumption of node homogeneity, where transmitters are modeled as stochastically identical, sharing the same signal strength, path-loss exponent, and activity probability. In Chapter 5, the model is extended by introducing a multi-tier network model, where nodes are grouped into classes distinguished by signal power and attenuation laws. However, this model assumes biased load balancing, resulting in equal stationary activity probabilities across tiers. Moreover, the input rate has been assumed homogeneous, with the same parameter p applied to all tiers. In practice, mobile networks exhibit significant heterogeneity: users experience varying path loss, fading, traffic demands, and mobility patterns [12, 34, 45]. Uplink transmissions are particularly sensitive to this variation due to limited coordination among user devices. To address this, recent studies have incorporated heterogeneity into network models. For example, [93] analyzes a lattice-based network of co-located transmitter-receiver pairs and derives stability conditions via analytical approximations. In contrast, [21, 22] examine abstract queuing networks with interference and state-dependent service rates. Namely, [22] develops a tractable framework to characterize stability under complex interference and dependent transmissions.

A key distinguishing feature of a heterogeneous interference model is that each interfering user impacts the performance of the transmitter in a non-uniform manner. This heterogeneity arises due to variations in several factors such as user location, transmission power, and channel conditions. For example, consider a user in a cellular network transmitting data using the LTE protocol. A device operating near the base station, but outside the intended cell, can cause significant inter-cell interference due to its proximity and possibly higher power level. In contrast, a device located at the cell edge or operating at lower power has a reduced impact on the network. In dense environments such as conference halls or airports, heterogeneity in device positions and power levels leads to unequal performance. To address such challenges, advanced interference coordination and user-aware scheduling mechanisms have been proposed. For example, [37] surveys heterogeneous and cognitive networks, and highlights systems in which nodes dynamically adjust transmission parameters.

To adapt our approach to the network with heterogeneous users and address the issues discussed above, the initially observed modeling framework is refined. In a new system, the homogeneity assumption is removed, such that each user is characterized by a set of random variables or deterministic

parameters that define their operational features. For this reason, certain performance metrics, for example, coverage probability, can vary across users and may depend on the state of the system or the local environment. Because the heterogeneity assumption is particularly relevant for mobile users, the primary focus of this section is the uplink network, where users serve as transmitters.

6.1 System model

The basic geometric framework remains the same as before, and the spatial stochastic model follows standard assumptions. Instead of treating the users locations as a random process, we consider a fixed realization of a PPP $\Phi_{UE}(\lambda_{UE})$. The Poisson-Voronoi framework applies, and each BS serves a corresponding Voronoi cell. Every user within a cell communicates with its associated BS via uplink transmission. The number of signals obtained by user $i, x_i \in \Phi_{UE}$ is $A_n^{(i)} \sim \text{Bin}(1, p_i)$. Here, p_i represents the i-th user input rate. A Rayleigh fading channel model is assumed, and the i-th user transmits the signal with strength $S_i \sim \exp(\mu_i)$, independently across users. The i-th user is associated with the buffer, storing failed transmissions. Similarly to the homogeneous model, the transmitting users interfere with each other, and the coverage probability depends on the active users. A crucial feature of a heterogeneous interference model is that each interfering user impacts the performance of the transmitter differently. For instance, an interferer located closer to the origin or transmitting with higher power has a substantially greater impact on the sender compared to those situated farther away or transmitting with lower power. Hence, to assess the network performance, it is no longer efficient to apply the mean-field approximation introduced in (4.3). For this reason, we develop a different framework and introduce the following notation of a *configuration*.

Let N denote the (fixed) total number of users within a typical cell. At time slot n, let $J_j(n)$ represent a random configuration comprising j active users, and denote by $\mathscr{C}_j(n)$ the ordered collection of all such possible configurations. Then

$$\mathscr{C}_j(n) = \left\{ J_j^{(1)}(n), J_j^{(2)}(n), \ldots, J_j^{\binom{N}{j}}(n) \right\},$$

where $J_j^{(k)}(n)$ is the k-th configuration. These configurations inherently account for the spatial positions of the active users. At each time slot, a typical BS experiences interference only from the users that are active in the current configuration $J_j^{(k)}(n)$. Then the interference experienced by user i at time n is given by

$$I^{(i)}(n) = \sum_{\substack{l \in J(n) \\ l \neq i}} S_l \, a(x_l), \tag{6.1}$$

where $J(n) := J_j^{(k)}(n)$ denotes the active set at time n. The path loss function $a(x_l)$ is defined as

$$a(x_l) = \frac{1}{\left|\frac{x_l}{r_0}\right|^{\beta}}. \tag{6.2}$$

For convenience, a typical BS is assumed to be positioned at the origin. The corresponding coverage probability is

$$P_c^{(i)}(J_n) = \mathbb{P}\left(\mathrm{SINR}^{(i)}(J_n) > T\right), \qquad \mathrm{SINR}^{(i)}(J_n) = \frac{S_i a(x_i)}{I^{(i)}(n) + \sigma^2}, \tag{6.3}$$

where the dependence on n comes from the interference $I^{(i)}(n)$, which in turn depends on the configuration $J(n)$.

6.2 Ergodicity of a buffer process

A mathematical representation of the buffer process in a heterogeneous network is, again, defined through the Lindley-type recursion. The network itself is viewed as a discrete-time stochastic system consisting of N interacting components. The state of component i at time slot n is denoted by $B_n^{(i)}$, representing a non-negative integer-valued queue length or buffer level. The evolution of the process for each component is given by the recursion

$$B_n^{(i)} = B_{n-1}^{(i)} + A_n^{(i)} - \mathbf{1}_{\{A_n^{(i)} + B_{n-1}^{(i)} \geq 1\}} \mathbf{1}_{\{S_i > T(\sigma^2/\mu + I^{(i)}(n))/a(x_i)\}}. \tag{6.4}$$

Let

$$\mathscr{B}_n = \{B_n^{(1)}, \ldots, B_n^{(N)}\}, \quad n \geq 1, \tag{6.5}$$

be the global system state that forms (due to the memoryless and stochastic structure of arrivals and services) a multi-dimensional Markov chain. Assuming that each component has a strictly positive probability of both receiving arrivals and successfully completing service in any slot, it can be shown that the Markov chain $\mathscr{B}_n$ is irreducible and aperiodic.

From the system setting, it is evident that the coverage probability (6.3) is generally non-increasing in the number of simultaneously active components. In other words, it reaches its maximum when all other components are idle, while the minimum occurs when all are active. Based on the general framework introduced in [22], the condition for the stability of component i has the form

$$\mathbb{E}[A_n^{(i)}] < P_c^{(i)}(J_{all}), \quad i = 1, \ldots, N, \tag{6.6}$$

where J_{all} denotes the configuration of a *fully loaded* system where all N components are simultaneously active. To interpret condition (6.6), consider a reference system where the service probability for each component is fixed at

$P_c^{(i)}(J_{all})$. Under such a static regime, if the arrival rate is strictly less than the fixed service probability, the buffer process is stochastically bounded, i.e., it is tight in probability. Moreover, by monotonicity arguments, the queue process in the reference system stochastically dominates the process $B_n^{(i)}$ in the original, state-dependent system. Therefore, tightness of the buffer process in the reference model implies tightness and hence stability of the original process, in the sense defined in [22].

Paper V provides stability analysis for the observed model, where conditions (6.6) are formulated and proved. The paper also includes a simulation study that validates the obtained conditions.

7. Multi-dimensional Markov chains

Building on the results from the previous chapter, simulations indicate that condition (6.6) becomes accurate when the number of active users approaches the total user population. However, when fewer users are active, the condition tends to overestimate the stability region, omitting a significant portion of the actual stable set. As a potential research direction, Paper VI suggests refining the stability condition through simulation-based methods inspired by [22]. This approach estimates the stationary distribution over system states via simulation and incorporates the results into an analytical framework to yield a more precise stability characterization. Such hybrid methods, however, introduce certain challenges. Empirical estimates are difficult to validate, and integrating them with analytical results can introduce interpretational and uncertainty issues due to the lack of a standard methodology. To overcome these limitations and derive fully analytical results, one must analyze a network model that explicitly incorporates queue dynamics. Given the birth-death structure of the buffer dynamics, a natural and effective approach is to model the system using multi-dimensional Markov chains.

Multi-dimensional Markov chains are stochastic processes whose state space consists of vectors in $\mathbb{Z}^d$ or $\mathbb{N}^d$, where $d \geq 2$. At each step, the process transitions between states according to a probability distribution that depends only on the current state, preserving the Markov property. While classical literature primarily addresses one-dimensional Markov chains (e.g., [67, Ch. 2,4], [64, Ch. III]), research on two-dimensional cases has also been widely developed. Early works such as [41, 40] link random walks with algebraic structures, while Li and Zhao [71] study multi-dimensional chains of M/G/1 type. Matrix-geometric methods are discussed in [84], and stability for a two-class retrial system is analyzed in [10], adapting conditions from [41]. Further results on discrete equations in the quarter-plane are provided by [77, 51]. Models with interacting queues on infinite grids are treated in [93, 16], the latter introducing heuristic methods with strong behavioral assumptions. When it comes to analytical results for three or more dimensions, the existing research is rather limited, mainly due to the analytical complexity of such models. An early contribution in this direction is [79], where conditions for ergodicity were proposed for the three-dimensional case ($n = 3$) and discussed more generally. While the approach is not fully rigorous and rests on structural assumptions that are difficult to verify, it provides one of the first attempts to extend such results beyond two dimensions.

The main challenge in analyzing the stability of an n-dimensional Markov chain is the dependence on the stationary distribution of its $(n-1)$-dimensional

marginal, which is itself typically unknown or analytically unavailable for $n > 2$. This dependency significantly complicates the analysis of stability conditions for higher-dimensional chains. As a result, obtaining exact analytical solutions for the stationary distributions of Markov chains in dimensions three and above remains an open and challenging problem. To address these limitations, various approximations have been proposed. The most relevant is the already discussed work [22], where the authors examine the ergodicity of n-dimensional MCs through a simulation-based framework. An important feature of their approach is the assumption of monotonicity of the transition rates of the queues, where the rates are assumed to be ordered in a non-decreasing manner.

To account for the limitations described above and as a natural extension of Paper IV, we propose an analytical framework for identifying stability conditions of a Markov chain of an arbitrary dimension.

7.1 Theoretical Tools

Before proceeding with the formulation of a buffered cellular network in terms of a multi-dimensional Markov chain, we recall the main analytical tools and definitions. Markov chains have been extensively studied as a fundamental class of stochastic processes. As a result, a wide theoretical framework has been developed to classify and understand their long-term behavior, particularly in terms of recurrence, transience, and ergodicity. Among the most important problems in Markov chain-related theory is the problem of its stability, that is, whether the chain tends to return to certain regions of the state space and remain there sufficiently often. In the discrete-time setting, the stability of a Markov chain on a countable state space is closely linked to positive recurrence. Classical results such as Foster's criterion provide necessary and sufficient conditions for positive recurrence using Lyapunov functions and drift inequalities. In addition, some other tools, usually based on the drift arguments, have been introduced to characterize systems that are null-recurrent or transient.

Let $\mathscr{X} = \{X_n\}_{n\geq 0}$ be a discrete-time Markov chain with countable state space $\mathscr{S}$ and transition matrix $P = (p(x,y))_{x,y\in\mathscr{S}}$. For any state $x \in \mathscr{S}$, define the *first return time* to x as

$$T_x := \inf\{n \geq 1 : X_n = x \mid X_0 = x\}.$$

The state x is said to be

(i) recurrent, if $\mathbb{P}_x(T_x < \infty) = 1$;

(ii) positive recurrent, if x is recurrent and $\mathbb{E}_x[T_x] < \infty$;

(iii) null recurrent if x is recurrent and $\mathbb{E}_x[T_x] = \infty$;

(iiii) transient, if $\mathbb{P}_x(T_x < \infty) < 1$.

In an irreducible Markov chain, these classifications are globally applied to all states: either all states are positive recurrent, all are null recurrent, or all are transient. A Markov chain is further classified as *positive recurrent* (or stable) if it is irreducible and all states $x \in \mathscr{S}$ are positive recurrent. Respectively, a Markov chain is said to be null-recurrent or transient if at least one state is null-recurrent or transient. The theoretical analysis of a Markov chain behavior generally distinguishes between the null-recurrent and transient states. However, in applied probability and performance analysis, stability typically refers to the existence of a stationary distribution and finite expected return times. Although a null recurrent chain returns to each state with probability one, the expected return time is infinite. In practical systems, such as queuing networks, communication protocols, or control processes, null recurrence becomes effectively indistinguishable from transience, where the system drifts away from bounded regions. Hence, both null recurrence and transience are treated as forms of instability, while positive recurrence is identified as stability. In this analysis, a Markov chain is considered *stable* if it is positive recurrent, and *unstable* if it is transient or null recurrent.

A classical result that provides necessary and sufficient conditions for the stability of a Markov chain is based on the construction of an appropriate Lyapunov function. This result is known as Foster's theorem and applies to any Markov process with a countable state space.

Theorem 1 (Foster's Theorem [43])**.** *Let $\mathscr{X} = \{X_n\}_{n\geq 0}$ be a discrete-time Markov chain with countable state space $\mathscr{S}$ and transition probabilities $p(x,y)$. Then $\mathscr{X}$ is positive recurrent if and only if there exists a function $f : \mathscr{S} \to \mathbb{R}$: $f(x) \geq 0$ for all $x \in \mathscr{S}$, a finite subset $\mathscr{F} \subset \mathscr{S}$, and a constant $\varepsilon > 0$ such that the following two conditions hold:*

(1) For all $x \in \mathscr{S} \setminus \mathscr{F}$, the expected drift satisfies

$$\sum_{y\in\mathscr{S}} p(x,y)f(y) \leq f(x) - \varepsilon.$$

(2) For all $x \in \mathscr{F}$, the expected value is finite:

$$\sum_{y\in\mathscr{S}} p(x,y)f(y) < \infty.$$

Foster's theorem is typically useful in cases where positive recurrence is the primary goal. However, it becomes non-informative when the system is not stable, as the failure to satisfy the positive recurrence conditions does not imply transience or null recurrence. In some applied settings, like the analysis of overloaded systems or critical regimes, detecting instability is crucial.

For example, in wireless networks with contention-based access mechanisms, such as ALOHA or CSMA, it is important to identify the maximal threshold beyond which the system becomes unstable to reach the highest efficiency of the protocol. For this reason, alternative Lyapunov-based criteria have been developed to provide sufficient conditions for instability. The most notable work is [41], where Theorem 2.2.6 provides an analysis of non-stable behavior of an MC under a bounded jump assumption. This result applies to both transient and null recurrent chains.

Theorem 2 (Instability Criterion [41, Theorem 2.2.6])**.** *The Markov chain* $\mathscr{X} = \{X_i, i = 0,1,\ldots\}$ *with state space* $\mathscr{S}$ *and transition probabilities* $p(\boldsymbol{x},\boldsymbol{y}) = P(X_i = x, X_{i+1} = y)$ *is not stable if there exists a Lyapunov function* $f : \mathscr{S} \longrightarrow \mathbb{R}$ *such that* $f(\boldsymbol{x}) \geq 0$, $\forall \boldsymbol{x} \in S$, *and there exist* $C, K < \infty$ *such that for* $\mathscr{F} = \{\boldsymbol{x} : \boldsymbol{x} \in \mathscr{S}, f(\boldsymbol{x}) \leq C\}$,

(1) $\sum_{\boldsymbol{y}\in S} p(\boldsymbol{x},\boldsymbol{y}) f(\boldsymbol{y}) \geq f(\boldsymbol{x}), \forall \boldsymbol{x} \in \mathscr{S} \setminus \mathscr{F}$

(2) $\sum_{\boldsymbol{y}\in S} p(\boldsymbol{x},\boldsymbol{y}) |f(\boldsymbol{y}) - f(\boldsymbol{x})| < K \forall x \in \mathscr{S}$.

A useful simplification of these conditions occurs when the set of states with negative drifts is finite. Formally, if the set $Z = \{x \in \mathscr{S} : \sum_{y\in\mathscr{S}} p(x,y) f(y) < f(x)\}$ is finite, then condition (1) in Theorem 2 is automatically satisfied by choosing an appropriate constant bounding constant C. More precisely, the choice $C = \max_{x\in Z} f(x)$ will directly guarantee instability.

The results above are stated for discrete-time Markov chains (DTMT), but they are applicable to continuous-time chains (CTMT) as well. As shown in [41, Section 1.3], if the holding times in a CTMT are uniformly bounded away from zero and infinity, or more generally if the total outgoing transition rates are uniformly bounded ([41, Formula 1.7]), then the embedded discrete-time chain and the original continuous-time process share the same stability classification. Therefore, all the results presented in this section may be directly applied to continuous-time processes under mild technical conditions. In the existing research, additional refinements and generalizations of these theorems can be found. For instance, the work by Meyn and Tweedie [80] studies stability and ergodicity for general Markov processes on general state spaces, extending the results stated above.

7.2 Buffered network with heterogeneous users as an N-dimensional MC

The physical model of the cellular network, as well as the spatial geometry of the cells, remains unchanged from the previous chapter. While modeling the user locations as a realization of a stochastic point process is suitable for capturing spatial randomness, it introduces significant complexity in the for-

mulation of a Markov chain model. This complexity arises from the randomness in the number of users, which conflicts with the requirement that the state space of the MC is deterministic in size. To address this issue, a conditional modeling approach can be adopted. Instead of modeling the users and BSs distributions as random objects, we fix a single realization of both the PPPs Φ_{UE} and Φ_{BS}. This allows for preserving the topology of the model, and the previously described methodology applies.

Let N denote the (fixed) total number of users in the network, corresponding to the number of points in the chosen realization of the PPP. Recall the retransmission model considered in the previous chapter, where the buffer dynamics of the user i is given by

$$B_n^{(i)} = B_{n-1}^{(i)} + A_n^{(i)} - \mathbf{1}_{\{A_n^{(i)}+B_{n-1}^{(i)}\geq 1\}} \mathbf{1}_{\{S_i > T(\sigma^2/\mu + I^{(i)}(n))/a(x_i)\}}, \tag{7.1}$$

see (6.4). As before, the activity comes from the signals obtained by users. Following the previous terminology, user i is active in slot n if $B_{n-1}^{(i)} > 0$ or $A_n^{(i)} > 0$, and inactive when $B_{n-1}^{(i)} = A_n^{(i)} = 0$. The global dynamics of all buffers in the network are given by the n-dimensional Markov chain

$$\mathscr{B}_n = \{B_n^{(1)}, \ldots, B_n^{(N)}\}, \quad n \geq 1, \tag{7.2}$$

with the state space $\mathscr{S} = \mathbb{N}^N$. The state space is partitioned into disjoint subsets $\mathscr{S}_{\mathbf{b}}$, indexed by binary vectors $\mathbf{b} \in \mathscr{B}_n = \{0,1\}^n$, representing activity state. In this notation, $b_i = 1$ means that the user i is active, and, respectively, $b_i = 0$ means that the user i is inactive. The state space is formally defined as

$$\mathscr{S}_{\mathbf{b}} = \{\mathbf{x} \in \mathbb{N}^n : x_i > 0 \text{ if } b_i = 1, \text{ and } x_i = 0 \text{ if } b_i = 0\}. \tag{7.3}$$

Let $p(\mathbf{x},\mathbf{y})$ denote the transition probability from state $\mathbf{x}$ to state $\mathbf{y}$. Because the buffer process of each user is a jump process, transitions are only allowed to states differing by a vector

$$\boldsymbol{\delta} \in \{-1,0,1\}^n,$$

hence

$$p(\mathbf{x},\mathbf{y}) = 0 \quad \text{unless } \mathbf{y} = \mathbf{x} + \boldsymbol{\delta} \text{ with } \boldsymbol{\delta} \in \{-1,0,1\}^n.$$

Within each activity class $\mathscr{S}_{\mathbf{b}}$, the behavior of the buffer process is symmetric in the sense that

$$p(\mathbf{x},\mathbf{x}+\boldsymbol{\delta}) = p(\mathbf{y},\mathbf{y}+\boldsymbol{\delta}) =: \pi_{\mathbf{b},\boldsymbol{\delta}}, \quad \forall \mathbf{x},\mathbf{y} \in \mathscr{S}_{\mathbf{b}},\ \mathbf{b} \in \mathscr{B}_n. \tag{7.4}$$

To assess the stability of a stochastic process, it is necessary to define and analyze its *drifts*. In the context of Markov chains, drift refers to the expected directional movement of the chain in the state space over time. More precisely, it characterizes whether the process tends to move toward or away from certain

regions of the state space. In the observed MC, the drift in the i-th coordinate under activity pattern $\mathbf{b}$ is defined as

$$d_{\mathbf{b},i} = \sum_{\boldsymbol{\delta}\in\{-1,0,1\}^n} \delta_i \pi_{\mathbf{b},\boldsymbol{\delta}}, \quad \forall i \in \{1,\dots,n\},\ \mathbf{b} \in \mathscr{B}_n. \tag{7.5}$$

A positive drift indicates that, on average, the buffer is increasing over time. Respectively, a negative drift indicates a decreasing trend in the buffer size. Due to the non-negativity of buffer states, transitions to negative values are infeasible, and hence are not allowed. Formally, on boundary states where $B_i(n) = 0$, the drifts are strictly positive,

$$d_{\mathbf{b},i} > 0, \quad \forall i \in \{1,\dots,n\},\ \mathbf{b} \in \hat{\mathscr{B}}_{n,i}, \tag{7.6}$$

where

$$\mathscr{B}_{n,i} = \{\mathbf{b} \in \mathscr{B}_n : b_i = 1\}, \quad \hat{\mathscr{B}}_{n,i} = \mathscr{B}_n \setminus \mathscr{B}_{n,i}.$$

7.3 Assumption of monotone drifts

A crucial setting that makes the stability analysis tractable for higher dimensions is the assumption of monotone drifts. In multi-dimensional Markov chains, such an assumption refers to the condition that the drift vectors are ordered across states. Specifically, for two states $x \le y$ (coordinate-wise), the drift satisfies

$$\mathbb{E}[X_{n+1} - X_n \mid X_n = x] \le \mathbb{E}[X_{n+1} - X_n \mid X_n = y].$$

Formally, for the observed MC, this condition is written as

$$d_{\boldsymbol{b},i} \le d_{\boldsymbol{c},i},\ \forall i \in \{1,\dots,n\}, \forall \boldsymbol{b},\boldsymbol{c} \in \mathscr{B}_{n,i} \text{ and } \boldsymbol{b} \le \boldsymbol{c}, \tag{7.7}$$

$$d_{\boldsymbol{b},i} \le d_{\boldsymbol{c},i},\ \forall i \in \{1,\dots,n\}, \forall \boldsymbol{b},\boldsymbol{c} \in \hat{\mathscr{B}}_{n,i} \text{ and } \boldsymbol{b} \le \boldsymbol{c}, \tag{7.8}$$

The use of assumptions (7.7)-(7.8) is motivated not only by the analytical traceability. In terms of coverage probability and input rates p_i, the drifts are written as

$$\begin{cases} d_{\mathbf{b},i} = p_i - P_c^{(i)}(\mathbf{b}),\ \forall b_i = 1; \\ d_{\mathbf{b},i} = p_i,\ \forall b_i = 0. \end{cases} \tag{7.9}$$

where $P_c^{(i)}(\mathbf{b})$ = is the coverage probability of user i given the global activity state $\mathbf{b}$. For example, in the case when $N = 3$ and $\mathbf{b} = \{1,0,1\}$, only users 1 and 3 are active. Then $P_c^{(1)}(\mathbf{b}) = P_c^{(1)}(\{1,0,1\})$ corresponds to the coverage probability of the first user, given that the users 1 and 3 are active, and only

they contribute to the interference. In the simple example with 3 users, the drift assumptions (7.8) and (7.7) imply that

$$\begin{cases} P_c^{(1)}(\{1,0,0\}) \geq P_c^{(1)}(\{1,0,1\}) \geq P_c^{(1)}(\{1,1,1\}); \\ P_c^{(2)}(\{0,1,0\}) \geq P_c^{(2)}(\{1,1,0\}) \geq P_c^{(1)}(\{1,1,1\}); \\ P_c^{(3)}(\{0,0,1\}) \geq P_c^{(1)}(\{1,0,1\}) \geq P_c^{(1)}(\{1,1,1\}). \end{cases}$$

Intuitively, it means that the coverage probability is maximized when no other users are active and minimized when all users are active. This behavior is natural and is based on physical characteristics of the system: as the number of active users increases, so does the aggregate interference, leading to a reduction in coverage probability. Conversely, when only a single user is active, it experiences zero interference, resulting in the highest possible SINR and consequently, the maximal coverage.

Paper VI presents an ergodicity analysis of the Markov chain with monotone drift structure and establishes both necessary and sufficient conditions for stability in arbitrary dimensions.

8. Dynamic optimization and reinforcement learning

Reinforcement Learning (RL) is a branch of machine learning that provides a collection of methods to study how agents learn to make decisions through interactions with an environment. In contrast to supervised and unsupervised learning, RL focuses on learning from consequences. RL terminology includes an agent, which is an object that makes decisions within the environment, state space, and action space. Typically, the main problem solved by RL is identifying a strategy (or policy) under which an agent chooses such actions that the cumulative long-term reward is maximized.

Formally, RL problems are often modeled as Markov Decision Processes (MDPs), characterized by a tuple $(\mathscr{S}, \mathscr{A}, P, r, \gamma)$, where $\mathscr{S}$ is the state space, $\mathscr{A}$ the action space, P the state transition probability, r the reward function, and $\gamma \in [0,1]$ the discount factor. At each step t, an agent observes the current state $s_t \in \mathscr{S}$, chooses an action $a_t \in \mathscr{A}$, receives a reward $r_t = r(s_t, a_t)$, and transitions to a new state $s_{t+1} \sim P(\cdot|s_t, a_t)$. The objective is to learn a policy $\pi(a|s)$ that maximizes the expected discounted return:

$$\mathbb{E}_\pi \left[\sum_{t=0}^{\infty} \gamma^t r(s_t, a_t) \right].$$

In many real-world problems, including wireless communication networks, multiple agents interact concurrently, making the environment non-stationary from any individual agent's perspective. This leads to the setting of multi-agent reinforcement learning (MARL). A MARL approach has been explored in several works, including [63, 114]. The study in [63] presents an extensive convergence analysis, establishing and proving sufficient conditions under which the learning dynamics converge. In contrast, [114] provides an overview of recent developments in decentralized MARL, particularly focusing on settings where agents are permitted to exchange information over a selected neighbor's set. This approach, however, becomes problematic as both the dimensionality of the state space and the number of agents increase. While the theoretical analysis applies regardless of the dimensions of the state and action spaces, the associated computational complexity grows rapidly, which results in practical implementation becoming nearly infeasible. A common approach to reduce the complexity of MARL is the mean-field approximation [113], where each agent interacts with the distribution of the states/actions of

the population rather than explicitly modeling all agent interactions. Mean-field MARL becomes particularly powerful when the state space and the number of agents are large and the interaction structure is symmetric. Under certain assumptions, the learning dynamics of each agent converges to a Nash equilibrium.

It turns out that a MARL approach fits particularly well within the field of wireless communications and cellular networks. Most modern wireless networks are decentralized and dynamic, with base stations and mobile devices making decisions in a state of uncertainty and with limited information. In an MARL framework, BSs act as agents and aim to choose an optimal policy to maximize the network performance. Such a framework allows individual agents to learn optimal policies through interaction with both the environment and other agents. A variety of studies have investigated the potential of MARL in the context of wireless communications. For instance, the use of MARL for distributed power control in interference-limited networks has shown improved energy efficiency and throughput [117]. Similarly, MARL-based techniques have been employed for dynamic spectrum access in cognitive radio networks, where agents can efficiently learn spectrum usage patterns and avoid collisions [103]. Furthermore, in ultra-dense networks, where user-cell association becomes increasingly complex, MARL offers a deep learning-based solution, an overview of which is given in [25].

8.1 Buffered Cellular Network in terms of MARL

As a new direction, the previously observed model of a buffered cellular network can be formulated in terms of a MARL model. The network topology and geometry of cells remain the same, and the Poisson-Voronoi framework applies. Now, the BS locations are assumed fixed and numerically available, representing a realization of a PPP. As before, each BS maintains a finite-capacity buffer and receives new signals at each time step with probability p. The BSs attempt to transmit buffered packets to associated users, and each transmission is subject to interference from active nodes. In cellular networks, a transmitting node generates interference that theoretically affects all cells, but signal attenuation causes this interference to decay with distance. As a result, distant stations are naturally shielded, and their contribution to overall interference becomes negligible. For this reason, the theoretical analysis often restricts attention to neighboring base stations, since they experience the most significant interference. In the Poisson-Voronoi setting, the neighbors are cells that share at least one common edge. Formally, for a BS located at $x \in \Phi_{BS}$, the corresponding Voronoi cell is

$$V(x) = \left\{ y \in \mathbb{R}^2 : \|y - x\| \leq \|y - x'\|, \forall x' \in \Phi_{BS} \right\}.$$

Respectively, the set of users associated with the BS located at x is defined as

$$C(x) = \left\{ y \in \Phi_{UE} : \|y - x\| \leq \|y - x'\|, \forall x' \in \Phi_{BS} \right\}.$$

The communication graph $G = (V, E)$ among BSs is defined via the adjacency of Voronoi cells: two BSs $x, x' \in \Phi_{BS}$ are communicative neighbors if their Voronoi cells $V(x)$ and $V(x')$ share at least one boundary. This corresponds to the Delaunay graph, the dual of the Voronoi tessellation [56]. The set of neighbors of agent i is given by

$$\mathcal{N}_i = \{ x \in \Phi_{BS} : V(x_i) \cap V(x) \neq 0 \}. \tag{8.1}$$

With this setting, the interference now comes only from the active nodes belonging to the neighbors set and is computed as

$$I_i = \sum_{x_j \in \mathcal{N}_i} S_j a(x_j, y_i) Q_j, \quad Q_j \sim \text{Bin}(1, q_j).$$

where

$$a(x_i, y_i) = \frac{1}{\|x - y\|^{\beta}}, \quad \beta > 2, \quad x_i \in \Phi_{BS}, \quad y_i \in C(x_i), \tag{8.2}$$

is the attenuation function similar to (3.6). It is worth noting that (8.2) provides a more precise representation of path loss, as it accounts for both the location of the base station and that of the user. This setting contrasts with the earlier formulation in (3.6), where the receiver was assumed to be fixed at the origin for the sake of analytical tractability. This model works fairly well from the analytical perspective and indeed simplifies the theoretical derivations. The RL framework, however, is based on numerical learning algorithms, where analytical traceability does not play a crucial role. For this reason, the signal attenuation function is reformulated in the form of (8.2) to account for the precise distance between a transmitter and a receiver. The average Shannon capacity is defined as

$$C_i = \mathbb{E}[\log_2(1 + \text{SINR}_i)] = \mathbb{E}\left[\log_2 \left(1 + \frac{S_i a(x_i, y_i)}{I_i + \sigma^2} \right) \right],$$

where $S_i = \min(Y_i, S_{max}, Y_i \sim \exp(\mu_i))$ is a signal strength, and μ_i is the controllable parameter. In case of an unsuccessful transmission, a signal from the i-th BS is sent to its respective buffer B_n^i, updated according to a Lindley-type recursion (4.6).

To dynamically optimize the network's performance, a MARL formulation is adopted. Each BS i is modeled as an agent that acts independently and interacts with its neighbors belonging to the set $\mathcal{N}_i$. Each agent's state space is defined as $\mathcal{S} = \{0, 1, \ldots, K\}$, where a state $s_i(n) \in \mathcal{S}$ represents the user's buffer length B_i at time n. The action space is $\mathcal{A} = \{\mu_1, \mu_2, \ldots, \mu_M\}$, where

each action $\mu \in \mathscr{A}$ determines the transmission intensity, i.e., the rate parameter of a truncated exponential distribution for signal power. The transition kernel is defined as

$$\mathscr{P}(b' \mid b, \mu) = \mathbb{P}\left(B_{n+1}^i = b' \mid B_n^i = b, \mu_i(n) = \mu\right).$$

Hence, all agents have identical state and action spaces, but each maintains its own independent sequence of state transitions and actions. Instead of QD-learning, which assumes a global state-action space and centralized control, a mean-field game (MFG) framework is employed, so each BS is treated as an agent interacting with the population's average behavior. The formulation partially follows the approach in [113]. The goal of each agent i is to maximize the reward function

$$r_i = C_i - \lambda_i B_n^i, \tag{8.3}$$

where λ_i is some penalty. The idea is to choose the appropriate signal strength μ_i such that the long-term capacity is maximized, while keeping the buffer sizes at a lower level.

8.2 Convergence

Each agent i independently applies Q-learning based on its local state and the mean-field distribution. Given the average action $\bar{\mu}_i$ observed by i-th agenet's neighbors and the value function $v_n^i(s')$ of the next state, the Q-function of agent i is updated as

$$Q_{n+1}^i(s, \mu_i, \bar{\mu}_i) = (1-\alpha)\, Q_n^i(s, \mu_i, \bar{\mu}_i) + \alpha\left[r^i + \gamma v_n^i(s')\right]. \tag{8.4}$$

with learning rate α_n and discount factor $\gamma \in [0,1]$. Convergence of the Q-function (8.4) in the mean-field RL setting requires some properties discussed in [113]. First, the state and action spaces have to be finite, the cost function should be bounded, and each state-action pair (s,a) should be visited infinitely often. Second, the policy must satisfy the Greedy in the Limit with Infinite Exploration (GLIE) condition. Third, the learning rate sequence $\{\alpha_n\}$ should meet the standard conditions: $\sum \alpha_n = \infty$ and $\sum \alpha_n^2 < \infty$. Finally, there should exist a Nash or saddle-point equilibrium for each stage game defined by the Q-values. If the convergence conditions are fulfilled, the approach is valid for optimizing the long-term performance of the cellular network model.

Paper VII provides a proper mean-field MARL formulation for the observed model, the formal proof of the convergence of Q-function, and implementation of the model using three algorithms: tabular Q-learning, deep Q-network (DQN), and myopic (baseline). Numerical results indicate a high efficiency of the DQN implementation compared to the tabular and myopic approaches.

9. Summary of papers

9.1 Paper I

The first paper introduces a stochastic geometric model for analyzing retransmission performance in downlink wireless cellular networks. The network is modeled using independent PPP for uses and BSs, forming a spatial structure of Poisson-Voronoi tessellation. Signal propagation is modelled by Rayleigh fading. The crucial feature is the incorporation of finite-capacity buffers at the transmitter side to handle failed transmissions, introducing queue dynamics. The main goal of the paper is to analyze system performance in terms of throughput, delay, and loss probability under this setup.

The BSs transmit signals with a signal power $S_i \sim \exp(\mu)$ during discrete time slots. The signal power is subject to distance-dependent attenuation, represented by a function

$$a_\beta(x) = \frac{\kappa+1}{\kappa+|\frac{x}{r_0}|^\beta},$$

where x is the distance between a user and its associated BS. The interference experienced by a typical user is modeled as a normalized interference field, focusing on signals within a d-dimensional ball $B(0,r_0)$ of the average size of a typical Voronoi cell. The total interference $I(\lambda)$ represents the cumulative effect of signals from other nodes in the network The first research contribution provided in the paper is the closed-form expression for downlink coverage probability, which is given by

$$V_T(q) = \int_0^\infty q\exp\left\{-\frac{\mu T\sigma^2(\kappa+v^\delta)}{1+\kappa} - q\int_v^\infty \frac{wT(\kappa+v^\delta)}{\kappa+u^\delta+T(\kappa+v^\delta)}du\right\}e^{-v}dv, \tag{9.1}$$

where $\delta = \beta/d$, T is the SINR threshold, and $w = \lambda_0/\lambda_1$ is the average number of users per cell. The dynamics of buffered retransmissions are modeled as a non-homogeneous Markov chain, with the buffer equation defined through a Lindley-type recursion. An iterative method is proposed to compute the steady-state busy-link probability q^* via the recursion

$$q_{n+1} = 1-(1-p)\nu_0^{(n)},$$

where $\nu_0^{(n)}$ is the stationary probability of the buffer being empty at time n. The core idea of identifying the buffer distribution is to fix time slot n and

associate with it a homogeneous MC defined by $\nu_k^{(n)}, k = 1, \ldots, K$. Then this auxiliary MC is ergodic and has a stationary distribution, due to its analytical properties, and the distribution is analytically available from the theory of birth-and-death processes. To show the convergence of the MC B_n, the convergence (4.11) has to be verified. In turn, to verify convergence (4.11), we first show the convergence of the sequence q_n. This convergence is proved based on the analytical properties of the coverage expression (9.1), and the limit q^* characterizes the long-term activity probability. The theoretical results are verified by simulation.

9.2 Paper II

The next paper features the same model of a buffered cellular network and builds on a stochastic geometric framework introduced in Paper I. The main focus of this paper is evaluating the channel capacity of a network in terms of Shannon's formula. The physical system coincides with the one described in Paper I, and the same stochastic geometry and Poisson-Voronoi methods apply. The expected Shannon capacity is defined as

$$\mathrm{Cap}_K(p,w) = \frac{w}{\ln 2} \int_0^{T_{\max}(p,w)} \frac{V_t(q_n)}{1+t} dt,$$

where $T_{\max}(p,w)$ is the maximal SINR such that $V_t(q^*) = p$ has a solution. As a novel performance metric, the pair (p,w) is said to be within Shannon capacity if

$$\mathrm{Cap}_K(p,w) \geq pw.$$

Next, we introduce a scaling regime where $w \to \infty$, $p \to 0$, such that $c = pw$ is fixed. The main result of the paper is the limiting Shannon capacity $\mathrm{Cap}_K(c)$ and the maximal admissible intensity $c_{\max}$. Let

$$H_\delta(t) = \int_1^\infty \frac{du}{1+u^\delta/t}, \quad t > 0, \tag{9.2}$$

then the capacity and the admissible intensity are:
i) for the pure-loss model $K = 0$,

$$\mathrm{Cap}_0(c) = \frac{1}{\ln 2} \int_0^\infty \frac{c}{1+cH_\delta(t)} \frac{dt}{1+t},$$

with $c_{\max}$ the unique solution of

$$\frac{1}{\ln 2} \int_0^\infty \frac{1}{1+c_{\max}H_\delta(t)} \frac{dt}{1+t} = 1;$$

ii) for the loss and delay models with any finite buffer size $K \geq 1$,

$$\mathrm{Cap}_K(c) = c\log_2\big(1+T_{\max}(c)\big) + \frac{1}{\ln 2}\int_{T_{\max}(c)}^{\infty}\frac{dt}{H_\delta(t)(1+t)},$$

with $c_{\max}$ the solution c of

$$\log_2\big(1+T_{\max}(c)\big) + \frac{1}{c\ln 2}\int_{T_{\max}(c)}^{\infty}\frac{dt}{H_\delta(t)(1+t)} = 1;$$

iii) and for the no-loss model $K=\infty$,

$$\mathrm{Cap}_\infty(c) = c\log_2\big(1+T_{\max}(c)\big), \tag{9.3}$$

with $c_{\max} = 1/H_\delta(1)$. The model quantifies the impact of buffer size, retransmission policies, and network scaling on the Shannon capacity of a cellular network. The main contribution is a method for quantifying wether the system is "workable" (that is, within the Shannon capacity) or "non-workable", distinguishing only between pure-loss, limited loss, or no-loss regimes. We provide analytical tools for characterizing the admissible traffic-load regions and evaluating the capacity saturation under ultra-dense scaling and the generic limiting forms.

9.3 Paper III

This paper introduces a stochastic geometric model for multi-tier buffered cellular networks, with the goal to evaluate and compare the performance of multi-tier versus single-tier deployments. In the model, BSs of J different tiers, such as macrocells and microcells, are independently distributed according to Poisson point processes Φ_i with intensities λ_i. Each BS has a buffer and transmits with tier-dependent power $S \sim \exp(\mu_i)$, where

$$\mu_1 \le \mu_2 \le \cdots \le \mu_J.$$

The BS of the i-th tier is active with probability q_i. The activity probability is given by:

$$q_i = 1-(1-p)\mathbb{P}(B^{(i)}=0),$$

where $B^{(i)}$ is the number of buffered signals in a typical BS of tier i. Coverage probability for a tier-i BS is

$$V_{t_i}^{(i)}(\bar{q}) = \frac{q_i}{1+w\sum_{j=1}^{J}\alpha_j q_j H_\delta(t_i\mu_i/\mu_j)},$$

where α_j is the association probability to tier j and $\delta = \beta/d$. The paper introduces an important assumption of *biased load balancing*, which is formally defined as

$$t_i\mu_i = t_1\mu_1.$$

for all $i = 1, \ldots, J$. Then the coverage probability becomes identical across all tiers

$$V_{t_i}^{(i)}(\bar{q}) = V_{t_1}^{(1)}(\bar{q}) = \cdots = V_{t_J}^{(J)}(\bar{q}).$$

The Shannon capacity of the network is defined as

$$\mathrm{Cap}_K^{(J)}(p, w) = w \sum_{i=1}^{J} \alpha_i \mathbb{E}[\log_2(1 + \mathrm{SIR}^{(i)})],$$

and under the no-loss assumption ($K = \infty$), this simplifies to

$$\mathrm{Cap}_\infty^{(J)}(p, w) = pw \log_2(1 + T_{\max}^{(J)}(p, w)),$$

where $T_{\max}^{(J)}(p, w)$ is the largest threshold for which the system balance equation holds.

The analysis shows that multi-tier systems, under biased load balancing and suitable parameter tuning (e.g., increasing tier density and adjusting power), outperform single-tier systems in both coverage and Shannon capacity. The second contribution of the paper introduces the notation of tier-specific pathloss, so that the signal from the BS of the i-th tier attenuates according to the law

$$a_i(x) = \frac{1}{||x||^{\beta_i}},$$

where

$$\beta_1 < \beta_2 < \ldots, < \beta_J.$$

With this setting, the performance further improved, as smaller cells with higher path loss attenuate interference more effectively. Simulations validate the theoretical predictions and show that the gain in multi-tier systems is robust across buffer regimes (pure loss, finite loss, and no loss).

9.4 Paper IV

The primary focus of this paper is on analyzing an uplink cellular network by examining a typical cell. The paper introduces a stochastic geometric framework to evaluate system performance in terms of signal coverage, interference, and buffer management. The contributions of this work include the stochastic analytical model of a buffered cellular network with uplink traffic and formulation of a necessary stability condition for the system, which is expressed in terms of the user activity factor, input rate p, and threshold T. The work is supported by an extensive simulation study which aims to validate the analytical stability condition. Additionally, the simulation study presents a heuristic condition that provides a more accurate stability zone under realistic scenarios, addressing the limitations of the derived stability condition.

The system model remains unchanged, and the focus is made on the uplink transmission policy. The coverage probability is derived for the simplest case when $\sigma^2 = \kappa = 0$ as

$$\begin{aligned} \mathsf{P}_\lambda(\mathrm{SINR}_i > T) &= \mathsf{P}\left(\frac{S_i a_\beta(x_i)}{I(\lambda)+\sigma^2} > T\right) \\ &= \mathbb{E}\left[e^{-\mu T(I(\lambda)+\sigma^2)/a_\beta(x_i)}|\cdot\right]. \end{aligned} \tag{9.4}$$

Expression (9.4) is the key formula in information theory and telecommunication engineering as it provides a crucial assumption about signal quality based on the relation between signal strength and external noise. Further analysis of (9.4) leads to several important findings regarding network stability. A necessary stability condition is derived, providing an upper bound of the activity factor p in relation to other model parameters, such that

$$p < p_c = \frac{1}{1+(\lambda_0/\lambda_1)C},\ C = K_\delta T^{1/\delta}, \tag{9.5}$$

where

$$K_\delta = \int_0^\infty \frac{dv}{1+v^\delta} = \frac{\pi/\delta}{\sin(\pi/\delta)}. \tag{9.6}$$

The simulation study investigates the users stability and provides validation of condition (9.5). In the simulation framework, the stability is analyzed based on the long-term buffer dynamics. Namely, a user is deemed stable if its buffer shows decreasing or non-increasing dynamics in the long run. The results reveal that condition (9.5) ensures stability of a limited fraction of users. That is, some users consistently remain unstable even when (9.5) holds. To adapt our analysis to more realistic scenarios and account for the complexities of user behavior and interference patterns, we propose a heuristic condition

$$p < \frac{1}{1+CN},\ C = K_\delta T^{1/\delta}, \tag{9.7}$$

where N is the number of users in a given cell estimated by simulation. It is important to note that the bound given by (9.7) cannot be obtained analytically as N is the sample value of a random variable $\xi \sim Poi(\lambda_0/\lambda_1)$. In the simulation framework, condition (9.7) appears to provide a more precise stability zone.

9.5 Paper V

The paper considers a slotted-time uplink cellular network with heterogeneous users and unlimited signal retransmissions, the network topology remains the same setting as before. All users are now distinguished by the input rate p_i

and signal power μ_i. The buffer size in slot n depends on the number of failed transmissions, which is determined by the transmission (coverage) probability. Let N be the total number of users. Let $J_j(n)$ be a random configuration of j active users in slot n, and $\mathscr{C}_j(n)$ the set of all such configurations (e.g., $\{1,2\}$ and $\{3,5\}$ are distinct). Let $J_j^{(k)}(n)$ denote the k-th element of the ordered set

$$\mathscr{C}_j(n) = \{J_j^{(1)}(n), \ldots, J_j^{(C_N^j)}(n)\},$$

where C_N^j is the number of j-combinations from N. Finally, let $P_c^{(i)}(\mathbf{0})$ and $P_c^{(i)}(\mathbf{N})$ denote the stationary configurations with only user i active and with all N users active, respectively.

The interference experienced by user i at time slot n comes from all active users belonging to the current configuration $J(n)$, so

$$I^{(i)}(n) = \sum_{l \in J(n), l \neq i} S_l a(x_l),$$

with $a(x_l)$ being the pathloss, S_l being exponentially distributed signal power, and $J(n)$ the set of active users in slot n. The coverage probability for user i is

$$P_c^{(i)}(n) = \mathbb{P}(\text{SINR}^{(i)}(n) > T) = e^{-T\sigma^2\mu_i|\frac{x_i}{r_0}|^\beta} \prod_{l \in J(n)} \frac{1}{1+T|\frac{x_l}{r_0}|^\beta}.$$

A Markov chain model is used to describe the evolution of each user's buffer. The main theoretical contribution is a relation connecting the steady-state input and output rates for user i:

$$p_i = \sum_{j=1}^{N} \sum_{k \in C_j} P_c^{(i)}(J_j^{(k)}) P_a^{(i)}(J_j^{(k)}),$$

where C_j is the set of configurations with j active users, $P_c^{(i)}(J_j^{(k)})$ is the coverage probability of user i under configuration $J_j^{(k)}$, and $P_a^{(i)}(J_j^{(k)})$ the corresponding stationary probability tat j active users compose configuration $J_j^{(k)}$. From this, a necessary condition for stability follows:

$$p_i \leq P_c^{(i)}(0),$$

and a sufficient condition adapted from [22] is

$$p_i < P_c^{(i)}(N).$$

Simulation results confirm that this sufficient condition is very close to being a stability criterion in heavily loaded networks. Furthermore, it is shown

that in less loaded network, this condition underestimates the stability region. Furthermore, the paper provides a recursive simulation-based method to refine stability bounds using estimates of stationary buffer distributions. The crucial assumption that allows this method to work is monotonicity of the coverage probabilities with respect to number of users. That is,

$$P_c^{(i)}(0) \geq P_c^{(i)}(1) \geq \ldots, \geq P_c^{(i)}(N).$$

9.6 Paper VI

The paper investigates the stability properties of n-dimensional discrete-time Markov chains with state space $\mathbb{N}^n$ and transition probabilities constrained by monotonic drift conditions. The main goal is to derive general sufficient and necessary conditions for the ergodicity (positive recurrence) of such chains. While exact stability criteria are well known for the one- and two-dimensional cases, the extension to higher dimensions ($n \geq 3$) is challenging due to the lack of closed-form stationary distributions. We define the state space as a collection of subsets S_b, indexed by binary vectors $b \in \{0,1\}^n$, where $x \in S_b$ iff $x_i > 0$ if and only if $b_i = 1$. Transition probabilities are homogeneous within each S_b, and state changes are allowed only to neighboring states: $x \to x + \delta$ with $\delta \in \{-1,0,1\}^n$.

Although the theoretical model is not directly linked to wireless communications, its structural properties align closely with the physical characteristics of a buffered cellular network. A key concept is the monotonicity of the drift vector, which requires that the drift $d_{b,i}$ in direction i is non-decreasing in b, formally:

$$d_{b,i} \leq d_{c,i} \quad \text{for all } b \leq c \text{ (component wise).}$$

Using Foster-Lyapunov criteria, we establish the following sufficient condition for stability (Theorem 4):

If the drift $d_{1,i} < 0$ for all i, or for each i with $d_{1,i} \geq 0$ there exists $j \neq i$ such that $d_{1,j} < 0$ and

$$d_{1,i}d_{1-e_j,j} - d_{1,j}d_{1-e_j,i} < 0,$$

then the chain is stable. Furthermore, a necessary condition for instability (transience) is formulated and proved in Theorem 5:

If for some $i \neq j$ either $d_{e_i+e_j,i}, d_{e_i+e_j,j} > 0$, or $d_{e_i+e_j,i} \geq 0$, $d_{e_i+e_j,j} < 0$, and

$$d_{e_i+e_j,j}d_{e_j,i} - d_{e_i+e_j,i}d_{e_j,j} > 0,$$

then the chain is unstable

The approach generalizes the known results for two-dimensional Markov chains and provides analytic bounds for the stability region in higher dimensions. The monotonicity of drifts is a crucial assumption which makes the theoretical analysis tractable in higher dimensions. Theoretical results are

complemented by numerical results visualizing stability regions for three-dimensional systems.

9.7 Paper VII

This paper introduces a decentralized reinforcement learning framework to optimize buffered cellular networks, where BSs and users are modeled via Poisson Point Processes. Following the previous setting, each BS has a finite buffer and receives new data randomly, attempting to transmit it under interference from neighboring BSs, defined via Voronoi adjacency. To avoid full centralization, we adopt a mean-field multi-agent reinforcement learning (MF-MARL) approach. Each agent observes only its local state and estimates the behavior of its neighbors through empirical distributions of buffer states and actions.

The agents aim to maximize a reward function that balances signal quality and buffer delay:

$$r_i(b,\beta;p,\pi) = \mathbb{E}\left[\log_2\left(1+\frac{S_i a(x_i,y_i)}{I_i+\sigma^2}\right)\right] - \lambda_i B_n^i,$$

where S_i is the signal power, $a(x_i,y_i)$ is the path-loss function, I_i is the local interference, $B_i(n)$ is the current buffer size, and λ_i is the penalty. The key contribution is a Q-learning algorithm adapted to the mean-field setting, where each agent independently learns an optimal transmission strategy based on local information. In the paper, we prove convergence of the Q-function under standard reinforcement learning conditions and compare the three approaches: Myopic, tabular Q-learning, and a Deep Q-network (DQN). The results show that DQN consistently outperforms both tabular and myopic approaches, resulting in an improved long-term capacity and lower delays. Overall, this paper provides a scalable and tractable analytical method for optimizing transmission policies in a buffered network by using local observations and mean-field approximations. The analysis developed in Papers I,II is used to investigate the behavior of the cost function and to derive the necessary analytical properties of the expected Shannon capacity and prove algorithm's convergence.

10. Sammanfattning på svenska

Denna avhandling behandlar stokastiska modeller och analysmetoder för trådlösa cellulära nätverk med buffrade sändare, där retransmissioner, kapacitetsgränser och stabilitet står i centrum. Utgångspunkten är en stokastisk-geometrisk ramverk baserat på Poissonpunktprocesser och Voronoi-cellstrukturer, där både basstationer och mobilanvändare modelleras slumpmässigt. I Paper I introduceras en modell för nedlänken där buffertdynamik och återtransmissioner analyseras med hjälp av stokastik geometri och Markovkedjor. Det huvudresultatet är en sluten form av buffertfördelning, aktivitetssannolikhet och täckningssannolikheter. Detta möjliggör explicita resultat även för lustsannolikhet, fördröjning och genomströmning. I Paper II vidareutvecklas modellen för att studera nätverkets kanal kapacitet enligt Shannons formel, där olika buffertregimer (ren förlust, begränsad förlust och ingen förlust) karakteriseras och en metod för att avgöra om ett system är "fungerande" presenteras.

I Paper III generaliseras ramverket till flernivå-nätverk, där basstationer av olika typer samverkar. Resultaten visar att, under biased load balancing, sådana multi-tier system kan ge betydande förbättringar både i täckning och Shannonkapacitet jämfört med enkelnivå-nät. Fokus flyttas därefter till upplänken i Paper IV, där ett nödvändigt stabilitetsvillkor härleds utifrån användarens aktivitetsgrad, trafikhastighet och interferenströskel. Genom simuleringar föreslås även ett heuristiskt villkor som bättre fångar realistiska stabilitetszoner.

I Paper V behandlas heterogena användare med olika trafikhastigheter och sändkraft, samt oändliga buffertar. Här introduceras en analys baserad på täckningssannolikheter under olika interferenskonfigurationer, vilket leder till nödvändiga och tillräckliga villkor för stabilitet. Dessa villkor kompletteras av en rekursiv simuleringsmetod som förfinar stabilitetsgränserna. I Paper VI lämnas de direkta nätverksmodellerna och en mer generell teori för stabilitet hos flerdimensionella Markovkedjor utvecklas. Genom att anta monotona driftvillkor härleds både tillräckliga och nödvändiga kriterier för ergodicitet i högdimensionella system, vilket direkt kan tillämpas på cellulära buffertnät.

Slutligen introduceras i Paper VII ett decentraliserat förstärkningsinlärnings ramverk för att optimera överföringsstrategier i buffrade nät. Med hjälp av mean-field multi-agent Q-learning kan basstationer och användare, med endast lokal information, lära sig stabila och effektiva strategier som balanserar signalkvalitet och buffertfördröjning. Metoden jämförs med en girig strategi och visar förbättrad långsiktig prestanda.

11. Acknowledgments

I would like to thank my supervisor Ingemar Kaj for constant and patient supervision during these years. Thank you for starting up this PhD project and for your valuable contribution to our papers. Thank you for sharing your knowledge and experience with me, and for helping me grow as a researcher. For supporting me in my research visits and new research directions, and for guiding me back on track whenever I began to stray. For your interest in the new projects that I started and for your valuable comments and feedback. It has been a pleasure and a privilege being your colleague this whole time.

I also thank my second supervisor, Rolf Larsson, for our occasional statistics discussions and for the teaching experience we've shared for a few years. Although my main PhD project ultimately had little to do with statistics, I always appreciated having the opportunity to discuss statistics and teaching with you. Also, a special thanks for introducing me to Reza Belaghi, who had essentially become my third supervisor and a co-author.

Reza, thank you for introducing me to the field of survival analysis and medical statistics and sharing your expertise with me. Thank you for the time you dedicated to our countless meetings in the evenings and on weekends. Thank you for starting up our project on medical data analysis, which resulted in a whole new paper. This project has sparked my interest in medicine, which is now the main direction for my future career. During these years, you have become not just my colleague, but also a friend whom I can always turn to for support and guidance.

Thanks to my other colleagues at the Department of Mathematics, with whom I partially shared my PhD journey. Christoffer, thank you for being a nice office mate, and for our forest walks and fikas. And for helping me overcome my Swedish barrier - I have become fluent thanks to you. Milica and Anna, thank you for also being nice office mates and for our occasional chit-chat breaks. Thanks also to Joel, Matti, Darius, Anna S., and Denis, whose occasional fun conversations made my time here more enjoyable.

Special thanks go to my closest friends for their constant support throughout my PhD journey. Sasha, there is probably no one I talked to and laughed with more than I did with you, from endless complaints about Migrationsverket and grant applications to our late-night conversations about everything. Thank you for all the things you did for me, which I cannot even count; you certainly made my PhD journey much less stressful than it could have been. Mattias, Pedro, Maria, and Kristina - during these years, you have become a constant and integral part of my life. Thank you for our countless volleyball games,

gym and beach sessions, boxing, swimming, billiards rounds, hiking, long forest walks, movie nights, lunches and dinners, fun evenings at Williams and Interpool, and a million other activities we have shared. My time in Uppsala would not have been nearly as enjoyable without you, and I appreciate our friendship so much.

Thanks also to my northern friends Peder and Joakim for all the fun time we had in Umeå - studying in the library for hours, walking in the forest, cooking and playing video games, climbing at Iksu, and many other things. And for visiting me in Uppsala and always hosting me in Umeå - I am really grateful for friends like you.

Thanks to the amazing research group at the Technical University of Budapest, which hosted me twice, and with whom I had the pleasure of collaborating. Illés, András, and Miklós, thank you for your interest in my project idea and for making this idea into something bigger, which resulted in a new solid paper. For the time you dedicated to this project, and for your valuable skills and technique. It has been a pleasure working with you.

The next thanks go to yet another amazing research group NEO at Inria Sophia-Antipolis, France. Kostia, thank you for inviting and hosting me at Inria, for supporting my interest in reinforcement learning, and for your guidance during this work. I am beyond happy that the project we started is now a part of this thesis. Thanks to the rest of the group for creating an amazing social atmosphere at the department, for all the fun we had at work and at the beach, our volleyball games and pool parties. I've had the best time there, and that is thanks to you.

A special thanks to Alexander, the supervisor of my bachelor's and master's thesis, who introduced me to the world of science and with whom I've had my very first publication. I am grateful for everything I've learned from you, and I have always looked up to you - and always will.

Finally, I would like to say thank you to my amazing family for their endless love and belief in me throughout these years. To my dad, a brilliant scientist himself, who knows more about the PhD process than I could ever have imagined, for his countless pieces of advice, tips, and support. To my mom, who understands me better than anybody and who always knows just what to say, for the very same reason. To my genius brother Victor for his constant help with Python and for always having the time to look at my code and make it better. And of course, I would like to thank Alex - for your love and support and for always being there for me.

References

[1] M. Agiwal, A. Roy, and N. Saxena. Next generation 5g wireless networks: A comprehensive survey. *IEEE Communications Surveys & Tutorials*, 18:1–1, 02 2016.

[2] I. Amini and M. Baidas. Reliability-latency tradeoffs in random access ultra-reliable low-latency energy-harvesting 5g networks with finite blocklength codes. 09 2020.

[3] V. Anantharam. How large delays build up in a gi/g/1 queue. *Queueing Systems*, 5:345–367, 1989.

[4] J. Andrews, F. Baccelli, and R. Ganti. A tractable approach to coverage and rate in cellular networks. *IEEE Transactions on Communications*, 59:3122–3134, 2011.

[5] J. Andrews, H. Claussen, M. Dohler, S. Rangan, and M. Reed. Femtocells: Past, present, and future. *IEEE JOURNAL ON SELECTED AREAS IN COMMUNICATIONS*, 30, 04 2012.

[6] J. Arnau, I. Atzeni, and M. Kountouris. Impact of los/nlos propagation and path loss in ultra-dense cellular networks. In *2016 IEEE International Conference on Communications (ICC)*, pages 1–6, 2016.

[7] J. ARTALEJO and G. Falin. Standard and retrial queueing systems: A comparative analysis. *Revista Matemática Complutense, 2002*, 15, 01 2002.

[8] A. Asadi, Q. Wang, and V. Mancuso. A survey on device-to-device communication in cellular networks. *IEEE Communications Surveys & Tutorials*, 16, 10 2013.

[9] S. Asmussen. *Applied Probability and Queues*. Springer, 2003.

[10] K. Avrachenkov, E. Morozov, and R. Nekrasova. Stability analysis of two-class retrial systems with constant retrial rates and general service times. *Performance Evaluation*, 159:102330, 01 2023.

[11] F. Baccelli and B. Blaszczyszyn. On a coverage process ranging from the boolean model to the poisson voronoi tessellation with applications to wireless communications. Technical report, INRIA, 2000. RR-4019, `inria-00072622`.

[12] F. Baccelli and B. B. Blaszczyszyn. *Stochastic Geometry and Wireless Networks: Volume 1 Theory*, volume 3. 2009.

[13] F. Baccelli, M. Klein, M. Lebourges, and S. Zuyev. Stochastic geometry and architecture of communication networks. *J. Telecommun. Syst.*, 7(1):209–227, 1997.

[14] F. Baccelli and S. Zuyev. Stochastic geometry models of mobile communication networks. *Unpublished*, 1996.

[15] A. K. M. Baki, M. W. Absar, T. Rahman, and K. M. A. Ahamed. Investigation of rayleigh and rician fading channels for state of the art (soa) lte-ofdm communication system. In *2017 4th International Conference on Advances in Electrical Engineering (ICAEE)*, pages 325–329, 2017.

[16] S. Banerjee and A. Sankararaman. Ergodicity and steady state analysis for interference queueing networks, 2020. Unpublished manuscript.
[17] M. Behrooz, T. Svensson, G. Caire, and M. Zorzi. Fast harq over finite blocklength codes: A technique for low-latency reliable communication. *IEEE Transactions on Wireless Communications*, PP:1–1, 11 2018.
[18] M. Bennis, m. Debbah, and H. V. Poor. Ultrareliable and low-latency wireless communication: Tail, risk, and scale. *Proceedings of the IEEE*, 106:1834–1853, 10 2018.
[19] M. Bennis, S. M. Perlaza, P. Blasco, Z. Han, and H. V. Poor. Self-organization in small cell networks: A reinforcement learning approach. *Wireless Communications, IEEE Transactions on*, 12:3202–3212, 07 2013.
[20] N. Bhushan, J. Li, D. Malladi, R. Gilmore, D. Brenner, A. Damnjanovic, R. Sukhavasi, C. Patel, and S. Geirhofer. Network densification: The dominant theme for wireless evolution in 5g. *Communications Magazine, IEEE*, 52:82–89, 02 2014.
[21] T. Bonald, S. Borst, N. Hegde, M. Jonckheere, and A. Proutiere. Flow-level performance and capacity of wireless networks with user mobility. *Queueing Syst.*, 63:131–164, 12 2009.
[22] S. C. Borst, M. Jonckheere, and L. Leskelä. Stability of parallel queueing systems with coupled service rates. *Discrete Event Dynamic Systems*, 18(4):447–472, 2010.
[23] P. Brémaud. *Markov Chains: Gibbs Fields, Monte Carlo Simulation and Queues*. Springer-Verlag, New York, NY, 1999.
[24] C.-S. Chang and J. A. Thomas. Effective bandwidth in high-speed digital networks. *IEEE Journal on Selected Areas in Communications*, 13(6):1091–1100, 1995.
[25] M. Chen, U. Challita, W. Saad, C. Yin, and m. Debbah. Artificial neural networks-based machine learning for wireless networks: A tutorial. *IEEE Communications Surveys & Tutorials*, 10 2017.
[26] X. Chen, L. Jiao, W. Li, and X. Fu. Efficient multi-user computation offloading for mobile-edge cloud computing. *IEEE/ACM Transactions on Networking*, 24(5):2795–2808, Oct. 2017.
[27] S. Chiu, D. Stoyan, W. Kendall, and J. Mecke. *Stochastic Geometry and Its Applications*. Wiley, 2013.
[28] X. Chu, D. Lopez-Perez, I. Dd, and F. Gunnarsson. *Heterogeneous Cellular Networks: Theory, Simulation and Deployment*. 07 2013.
[29] P. Collet, S. Martinez, and J. San Martin. *Birth-and-Death Chains*, pages 69–111. 01 2013.
[30] F. Danufane and M. Di Renzo. Analysis of the delay distribution in cellular networks by using stochastic geometry. *IEEE Open Journal of the Communications Society*, PP:1–1, 2023.
[31] L. Decreusefond, I. Flint, and A. Vergne. Efficient simulation of the ginibre point process. *Journal of Applied Probability*, 52(4), 2015. ffhal-00869259v2f.
[32] N. Deng, W. Zhou, and M. Haenggi. The ginibre point process as a model for wireless networks with repulsion. *IEEE Transactions on Wireless Communications*, 14(1):107–121, 2015.
[33] H. S. Dhillon, R. K. Ganti, F. Baccelli, and J. G. Andrews. Modeling and

analysis of k-tier downlink heterogeneous cellular networks. *IEEE Journal on Selected Areas in Communications*, 30(3):550–560, 2012.

[34] H. S. Dhillon, R. K. Ganti, F. Baccelli, and J. G. Andrews. Modeling and analysis of k-tier downlink heterogeneous cellular networks. *IEEE Journal on Selected Areas in Communications*, 30(3):550–560, 2012.

[35] H. S. Dhillon, T. D. Novlan, and J. G. Andrews. Coverage probability of uplink cellular networks. In *2012 IEEE Global Communications Conference (GLOBECOM)*, pages 2179–2184, 2012.

[36] K. Dogbe and N. Hakem. Performance analysis of full-duplex relaying over rayleigh-rician fading channels. In *2019 USNC-URSI Radio Science Meeting (Joint with AP-S Symposium)*, pages 29–30, 2019.

[37] H. ElSawy, E. Hossain, and M. Haenggi. Stochastic geometry for modeling, analysis, and design of multi-tier and cognitive cellular wireless networks: A survey. *IEEE Communications Surveys & Tutorials*, 15(3):996–1019, 2013.

[38] J. G. A. et al. What will 5g be? *IEEE Journal on Selected Areas in Communications*, 32(6):1065–1082, 2014.

[39] A. Farzamnia, L. Zhen, and E. Moung. Efficient cellular network with network coding in disaster area. *Wireless Personal Communications*, 106, 05 2019.

[40] G. Fayolle, R. Iasnogorodski, and V. A. Malyshev. *Random Walks in the Quarter-Plane: Algebraic Methods, Boundary Value Problems and Applications*. Springer-Verlag, 1999.

[41] G. Fayolle, V. Malyshev, and M. Menshikov. *Topics in the constructive theory of countable Markov chains*. Cambridge university press, 1995.

[42] S. Foss and S. Zuyev. On a voronoi aggregative process related to a bivariate poisson process. *Adv. Appl. Probab.*, 28(4):965–979, 1996.

[43] F. G. Foster. On the stochastic matrices associated with certain queuing processes. *Annals of Mathematical Statistics*, 24(3):355–360, 1953.

[44] S. Fowler, C. Häll, D. Yuan, G. Baravdish, and A. Mellouk. Analysis of vehicular wireless channel communication via queueing theory model. In *2014 IEEE International Conference on Communications, ICC 2014*, 2014.

[45] R. K. Ganti and M. Haenggi. Interference and outage in clustered wireless ad hoc networks. *IEEE Transactions on Information Theory*, 55(9):4067–4086, 2009.

[46] X. Ge, H. Cheng, M. Guizani, and T. Han. 5g wireless backhaul networks: Challenges and research advance. *IEEE Network*, 28, 12 2014.

[47] G. Ghatak, A. De Domenico, and M. Coupechoux. Coverage analysis and load balancing in hetnets with millimeter wave multi-rat small cells. *IEEE Transactions on Wireless Communications*, 17(5):3154–3169, 2018.

[48] A. Ghosh, N. Mangalvedhe, R. Ratasuk, B. Mondal, M. Cudak, E. Visotsky, T. Thomas, J. Andrews, P. Xia, H.-S. Jo, H. Dhillon, and T. Novlan. Heterogeneous cellular networks: From theory to practice. *IEEE Communications Magazine - IEEE Commun. Mag.*, 50:54–64, 06 2012.

[49] K. S. Gilhousen, I. M. Jacobs, R. Padovani, A. J. Viterbi, L. A. Weaver, and C. E. Wheatley. On the capacity of a cellular cdma system. *IEEE Transactions on Vehicular Technology*, 40(2):303–312, 1991.

[50] J. Ginibre. Statistical ensembles of complex, quaternion, and real matrices. *Journal of Mathematical Physics*, 6(3):440–449, 03 1965.

[51] S. V. Grishin. Random walks on the line and algebraic curves. *Ufimsky Mathematical Journal*, 16(1):24–34, 2024.
[52] R. Guiazon, K.-K. Wong, and M. Fitch. Coverage probability of cellular networks using interference alignment under imperfect csi. *Digital Communications and Networks*, 2:162–166, 2016.
[53] P. Gupta and P. Kumar. Internets in the sky: capacity of 3d wireless networks. In *Proceedings of the 39th IEEE Conference on Decision and Control (Cat. No.00CH37187)*, volume 3, pages 2290–2295 vol.3, 2000.
[54] M. Haenggi. User point processes in cellular networks. *IEEE Wireless Communications Letters*, 6(2):258–261, 2017.
[55] M. Haenggi, J. G. Andrews, F. Baccelli, O. Dousse, and M. Franceschetti. Stochastic geometry and random graphs for the analysis and design of wireless networks. *IEEE Journal on Selected Areas in Communications*, 27(7):1029–1046, 2009.
[56] B. Hansen and T. Müller. Poisson-voronoi percolation in the hyperbolic plane with small intensities. *The Annals of Probability*, 52, 11 2024.
[57] H. Inaltekin, M. Chiang, H. V. Poor, and S. B. Wicker. On unbounded path-loss models: effects of singularity on wireless network performance. *IEEE Journal on Selected Areas in Communications*, 27(7):1078–1092, 2009.
[58] D. Ioffe. Stochastic geometry of classical and quantum ising models. *Lecture Notes in Mathematics*, 1970, 03 2009.
[59] D. L. Isaacson and R. W. Madsen. *Markov Chains: Theory and Applications*. John Wiley & Sons, Inc., New York, NY, 1976.
[60] M. Jabi, M. Benjillali, L. Szczecinski, and F. Labeau. Energy efficiency of adaptive harq. *IEEE Transactions on Communications*, 64:1–1, 01 2015.
[61] V. Jacobson. Congestion avoidance and control. In *Proceedings of ACM SIGCOMM*, pages 314–329, 1988.
[62] H.-S. Jo, Y. J. Sang, P. Xia, and J. G. Andrews. Heterogeneous cellular networks with flexible cell association: A comprehensive downlink sinr analysis. *IEEE Transactions on Wireless Communications*, 11(10):3484–3495, 2012.
[63] S. Kar, J. Moura, and H. V. Poor. *qd*-learning: A collaborative distributed strategy for multi-agent reinforcement learning through consensus + innovations. *IEEE Transactions on Signal Processing*, 61, 04 2012.
[64] S. Karlin and H. M. Taylor. *An Introduction to Stochastic Modeling*. Academic Press, 3rd edition, 1998.
[65] F. P. Kelly. *Reversibility and Stochastic Networks*. Cambridge University Press, 2011.
[66] L. Kleinrock. *Queueing Systems, Volume 1: Theory*. Wiley, 1975.
[67] V. G. Kulkarni. *Modeling and Analysis of Stochastic Systems*. CRC Press, 2010.
[68] R. Kumar, A. Francini, S. Panwar, and S. Sharma. Dynamic control of rlc buffer size for latency minimization in mobile ran. In *2018 IEEE Wireless Communications and Networking Conference (WCNC)*, pages 1–6, 2018.
[69] A. Larrañaga, M. d. C. Lucas-Estañ, I. Martinez, and J. Gozalvez. 5g nr configured grant in ns-3 network simulator for ultra-reliable low latency communications. *Procedia Computer Science*, 201:502, 04 2022.

[70] H. Lee, Y. Park, and D. Hong. Resource split full duplex to mitigate inter-cell interference in ultra-dense small cell networks. *IEEE Access*, 6:37653–37664, 2018.
[71] J. Li and Y. Q. Zhao. Multi-dimensional markov chains of m/g/1 type. *Mathematics*, 13(2):209, 2023.
[72] P. Li, M. Pan, and Y. Fang. The capacity of three-dimensional wireless ad hoc networks. In *2011 Proceedings IEEE INFOCOM*, pages 1485–1493, 2011.
[73] C. Lima, M. Bennis, and M. Latva-aho. Statistical analysis of self-organizing networks with biased cell association and interference avoidance. *IEEE Transactions on Vehicular Technology*, 62, 01 2013.
[74] J. Liu, M. Sheng, L. Liu, and J. Li. Effect of densification on cellular network performance with bounded pathloss model. *IEEE Communications Letters*, 21(2):346–349, 2017.
[75] W. Liu, G. Nair, Y. Li, D. Nesic, B. Vucetic, and H. V. Poor. On the latency, rate and reliability tradeoff in wireless networked control systems for iiot. *IEEE Internet of Things Journal*, pages 1–1, 2020.
[76] D. Lopez-Perez, I. Guvenc, G. Roche, M. Kountouris, T. Q. Quek, and J. Zhang. Enhanced inter-cell interference coordination challenges in heterogeneous networks. *IEEE Wireless Communications*, 18:22 – 30, 06 2011.
[77] V. A. Malyshev. On the solution of discrete wiener-hopf equations in the quarter-plane. *Doklady of the Academy of Sciences of the USSR*, 187(6):1243–1246, 1969.
[78] L. Marandi, M. Naslcheraghi, S. A. Ghorashi, and M. Shikh-Bahaei. Delay analysis in full-duplex heterogeneous cellular networks (open access). *IEEE Transactions on Vehicular Technology*, 68(10):9713–9721, 2019.
[79] M. V. Menshikov. Ergodicity and transience conditions for random walks in the positive octant of space. *Doklady Akademii Nauk SSSR*, 217(4):755–758, 1974.
[80] S. P. Meyn and R. L. Tweedie. *Markov Chains and Stochastic Stability*. Springer, London, 1993.
[81] N. Miyoshi and T. Shirai. A cellular network model with ginibre configured base stations. *Advances in Applied Probability*, 46, 09 2014.
[82] I. Moon, L. Dũng, and T. Kim. Optimal 3d placement of uav-bs for maximum coverage subject to user priorities and distributions. *Electronics*, 11:1036, 03 2022.
[83] A. Mouradian. Modeling dense urban wireless networks with 3d stochastic geometry. *Performance Evaluation*, 121-122:1–17, 2018.
[84] M. F. Neuts. *Matrix-Geometric Solutions in Stochastic Models: An Algorithmic Approach*. Dover Publications, 1981.
[85] T. Novlan, H. Dhillon, and J. Andrews. Analytical modeling of uplink cellular networks. *Wireless Communications, IEEE Transactions on*, 12:2669–2679, 2013.
[86] S. Oh, J. W. Song, W. Chang, and M. Lee. Estimation and forecasting of sovereign credit rating migration based on regime switching markov chain. *IEEE Access*, PP:1–1, 08 2019.
[87] A. Razzaque, H. Qureshi, and A. Baiocchi. Low vs high spectral efficiency

communications with sic and random access. pages 1–6, 11 2022.
[88] RF Wireless World. Uplink vs downlink: Key differences in wireless communication. `https://www.rfwireless-world.com/terminology/uplink-vs-downlink`, 2025.
[89] S. O. Rice. Mathematical analysis of random noise. *Bell System Technical Journal*, 24(1):46–156, 1945.
[90] E. Sabir. Generalized slotted aloha with partial information revisited: A throughput and stability analysis. 09 2015.
[91] G. Sallai. Optimum network structure with randomly distributed nodes. In *12th International Teletraffic Congress (ITC), Volume No. 2.1, B-4, p.9*, 1988.
[92] A. Sankararaman and F. Baccelli. Spatial birth-death wireless networks. *IEEE Transactions on Information Theory*, pages 1–1, 2017.
[93] A. Sankararaman, F. Baccelli, and S. Foss. Interference queueing networks on grids, 2020. Unpublished manuscript.
[94] P. Schulz et al. Latency critical iot applications in 5g: Perspective on the design of radio interface and network architecture. *IEEE Communications Magazine*, 55(2):70–78, Feb. 2017.
[95] L. I. Sennott et al. Mean drifts and the non-ergodicity of markov chains. *Operations Research*, 31(4):783–789, 1983. Accessed 21 Feb. 2025.
[96] B. Sericola. *Markov Chains*, pages 191–233. 08 2013.
[97] C. E. Shannon. A mathematical theory of communication. *Bell System Technical Journal*, 27(3):379–423, 1948.
[98] O. Simeone, O. Somekh, H. V. Poor, and S. Shamai. Local base station cooperation via finite-capacity links for the uplink of linear cellular networks. *IEEE Transactions on Information Theory*, 55:190–204, 2009.
[99] B. Sklar. Rayleigh fading channels in mobile digital communication systems. i. characterization. *IEEE Communications Magazine*, 35(9):136–146, 1997.
[100] B. Sklar. Rayleigh fading channels in mobile digital communication systems part ii: Mitigation. *IEEE Communications Magazine*, 35:148–155, 1997.
[101] D. Stoyan and G. Lippmann. Models of stochastic geometry - a survey. *ZOR - Methods and Models of Operations Research*, 38(3):235–260, 1993.
[102] S. Sun, T. A. Thomas, T. S. Rappaport, H. Nguyen, I. Z. Kovacs, and I. Rodriguez. Path loss, shadow fading, and line-of-sight probability models for 5g urban macro-cellular scenarios. In *2015 IEEE Globecom Workshops (GC Wkshps)*, pages 1–7, 2015.
[103] X. Tan, L. Zhou, H. Wang, Y. Sun, H. Zhao, B.-C. Seet, J. Wei, and V. C. M. Leung. Cooperative multi-agent reinforcement-learning-based distributed dynamic spectrum access in cognitive radio networks. *IEEE Internet of Things Journal*, 9(19):19477–19488, 2022.
[104] X. Tang, P. Ren, Y. Wang, Q. Du, and L. Sun. User association as a stochastic game for enhanced performance in heterogeneous networks. In *2015 IEEE International Conference on Communications (ICC)*, pages 3417–3422, 2015.
[105] P. Vassiliou. *Non-Homogeneous Markov Chains and Systems: Theory and Applications*. 11 2022.
[106] B. N. Vellambi, N. Torabkhani, and F. Fekri. Throughput and latency in finite-buffer line networks. *IEEE Transactions on Information Theory*,

57(6):3622–3643, 2011.
[107] A. J. Viterbi, A. M. Viterbi, and E. Zehavi. Other-cell interference in cellular power-controlled cdma. *IEEE Transactions on Communications*, 42(234):1501–1504, February/March/April 1994.
[108] J. Wang, J. Cao, and Q.-L. Li. Reliability analysis of the retrial queue with server breakdowns and repairs. *Queueing Syst.*, 38:363–380, 08 2001.
[109] W. Whitt. Tail probabilities with statistical multiplexing and effective bandwidths in multi-class queues. *Telecommunication Systems*, 2:71–107, 1993.
[110] A. D. Wyner. Shannon-theoretic approach to a gaussian cellular multiple-access channel. *IEEE Transactions on Information Theory*, 40(6):1713–1727, 1994.
[111] J. Xu, J. Zhang, and J. Andrews. When does the wyner model accurately describe an uplink cellular network? In *GLOBECOM 2010, 2010 IEEE Global Telecommunications Conference*, pages 1–5, 2011.
[112] X. Yang and A. O. Fapojuwo. Coverage probability analysis of heterogeneous cellular networks in rician/rayleigh fading environments. *IEEE Communications Letters*, 19(7):1197–1200, 2015.
[113] Y. Yang, R. Luo, M. Li, M. Zhou, W. Zhang, and J. Wang. Mean field multi-agent reinforcement learning. In *International conference on machine learning*, pages 5571–5580. PMLR, 2018.
[114] K. Zhang, Z. Yang, and T. Başar. Decentralized multi-agent reinforcement learning with networked agents: Recent advances. *Frontiers of Information Technology & Electronic Engineering*, 22(6):802–814, 2021.
[115] X. Zhang and J. Andrews. Downlink cellular network analysis with multi-slope path loss models. *IEEE Transactions on Communications*, 63, 2014.
[116] X. Zhang and M. Haenggi. The performance of successive interference cancellation in random wireless networks. *IEEE Transactions on Information Theory*, 60(10):6368–6388, 2014.
[117] N. Zhao, Z. Liu, and Y. Cheng. Multi-agent deep reinforcement learning for trajectory design and power allocation in multi-uav networks. *IEEE Access*, 8:1–1, 01 2020.

Acta Universitatis Upsaliensis

Digital Comprehensive Summaries of Uppsala Dissertations from the Faculty of Science and Technology 2615

Editor: The Dean of the Faculty of Science and Technology

A doctoral dissertation from the Faculty of Science and Technology, Uppsala University, is usually a summary of a number of papers. A few copies of the complete dissertation are kept at major Swedish research libraries, while the summary alone is distributed internationally through the series Digital Comprehensive Summaries of Uppsala Dissertations from the Faculty of Science and Technology. (Prior to January, 2005, the series was published under the title "Comprehensive Summaries of Uppsala Dissertations from the Faculty of Science and Technology".)

Distribution: publications.uu.se
urn:nbn:se:uu:diva-571533

ACTA UNIVERSITATIS
UPSALIENSIS
2025